Pitch and Torque Control of Variable Speed Wind Turbines

ARKADIUSZ KULKA

Department of Electric Power Engineering
CHALMERS UNIVERSITY OF TECHNOLOGY
Göteborg, Sweden 2004

THESIS FOR THE MASTER OF SCIENCE DEGREE

Pitch and Torque Control of Variable Speed Wind Turbines

Arkadiusz Kulka

Department of Electric Power Engineering
CHALMERS UNIVERSITY OF TECHNOLOGY
Göteborg, Sweden 2004

Titel
Moment, varvtals- och pitchreglering av vindkraftverk

Title in english
Pitch and Torque Control of Variable Speed Wind Turbines

Författare/Author
Arkadiusz Kulka

Utgivare/Publisher
Chalmers tekniska högskola
Institutionen för elteknik
412 96 Göteborg, Sverige

ISSN
1401-6184

Examensarbete/M.Sc. Thesis No.
100E

Ämne/Subject
Högspänningsteknik

Examinator/Examiner
Torbjörn Thiringer

Datum/Date
2004-06-25

Tryckt av/Printed by
Chalmers tekniska högskola
412 96 GÖTEBORG

Abstract

In this thesis the torque, speed and pitch angle control of variable speed wind turbine is investigated. In particular, it concentrates on the extraction of maximum available energy, reduction of torque and output power variations, which gives stresses in the gearbox and mechanical structure. The control concentrates on separate wind speed internals as well as on whole wind speed region. It is found that the control structures varies substantially between the wind speed regions. Finally the result are compared with measurement made on 2 variable speed turbines.

Keywords: *Wind turbine, pitch control, variable speed operation, torque control, mechanical stresses, energy capture.*

Acknowledgments

First of all I would like to thank my supervisor at Chalmers University of Technology, Assoc. Prof. Torbjörn Thiringer for invaluable and endless discussions about control issues.

I am grateful to all the staff at the department of Electrical Power Engineering especially, Magnus Ellsen for helping me with the measurement, Andreas Petersson and Oskar Wallmark for interesting discussion and for sharing the knowledge about LaTex system.

Finally, I would like to thank the whole department for making me feel welcome and for the nice working atmosphere during my stay in Sweden.

Arkadiusz Kulka
24th June 2004

Table of Contents

List of Symbols

Abbreviations

A_d	rotor swept area
C_P	power coefficient of rotor blades
V_{cut-in}	cut in wind speed for turbine
$V_{cut-off}$	cut off wind speed for turbine
R	Rotor blade radius
ρ	air density
ω_r	rotor shaft speed [rad/sek]
WS	wind speed
RSF	Rotational Sampling Filter
SF	Spatial Filter
DFIG	doubly-fed induction generator
EMF	electro motive force
IG	induction generator
IM	induction machine
PWM	pulse width modulation
SG	synchronous generator
I	low wind speed interval
II	middle wind speed interval
III	high wind speed interval
λ	tip speed ratio
α	attack angle
β	pitch angle of the blade
F_{lift}	lift force on blade segment
F_{drag}	drag force on blade segment
F_{thrust}	longitudinal force on rotor axis
F_{total}	total force on blade segment
P	active power
p	derivative operator
Q	reactive power

Chapter 1

Introduction

1.1 General Background

Using the wind is not a new idea. For hundreds of years, the famous Dutch windmills have faithfully pumped water, keeping land reclaimed or grinding grain. Today, the windmill's modern equivalent - a wind turbine, uses the energy in the wind to generate electricity. In the 19th century the first wind turbine for electricity generation came into use, constructed by Charles Brush (inventor of several key technologies in the electrical industry). The turbine was 17 meters tall and had 144 cedar made rotor blades. Soon thereafter, Poul la Cour, a Dane, discovered that fast rotating wind turbines with fewer rotor blades generated electricity more efficiently than a slowly rotating wind turbines with many rotor blades. This opened the door to a number of wind turbine advances during the 20th century.

Wind power is the world's fastest growing source of electricity [8]. Generating capacity grew at an average annual rate of 25% between 1990 and 2000. At the end of 2002 the total global wind generating capacity exceeded 31,000 MW, and provides about 65 billion kWh of electricity annually. This is enough to meet the needs of over 6 million average American homes. The generating capacity is mainly concentrated in just five countries; Germany (36%), the U.S. (18%), Spain (14%), Denmark (10%) and India (6%). Wind electricity generation has been expanding rapidly during recent years, due to largely technological improvements, industry maturation and an increasing concern regarding the emissions associated with burning fossil fuels.

1.2 Problem Background

Automatic control is essential for efficient and reliable operation of wind power turbines and is an interesting, challenging research topic. Nowadays, variable speed wind turbines are becoming more common than constant speed turbines. This is mainly due to a better power quality impact, reduction of stresses in the turbine and the reduction of the weight and cost of the main components. The traditional fixed-speed turbines are stall regulated while the new, variable-speed turbines are pitch-regulated. The most commonly used parameter describing the relative rotor speed is $\frac{TipSpeed}{WindSpeed} = \lambda$. The aerodynamic efficiency $Cp(\lambda, \beta)$ is a function of the tip-speed ratio and the pitch angle β. Given a pitch angle, the efficiency coefficient C_p has a maximum for a certain tip-speed ratio, λ. It is thus obvious that to maximize the efficiency of the turbine, we should be able to vary its rotational speed to follow the wind speed. The fluctuating nature of the wind makes the variable speed turbine a nontrivial object to control. The objectives is to achieve high efficiency and at the same time have a smooth power output. The control variables are the electrodynamical torque and the pitch angle.

1.3 Previous Work

Although the control of variable speed pitch-controlled is an important area and obviously routines have been developed by manufacturers, there is not much to be found in the generally available literature. The steady-state operating conditions are well described by Bossanyi [2]. In Mika [22] suggestions for controllers for some wind speed regions can be found, however, no solutions of how to switch between these controllers were presented.Moreover, in Mika [22] the suggested pitch controller was of a very active type, that could lead to wear of the mechanical parts, which, of course, is a drawback.

1.4 Purpose of the thesis

The main purpose of this work is to design and analyze control algorithms for variable speed wind turbines with pitch angle control. Moreover a goal is to study the the trade-off between minimum of torque variations and maximum energy gain. Further, the objective is to make a controller structure that is valid in the whole wind speed region. In addition, another goal is to investigate a pitch controller that is much less active which could lead to reduced mechanical wear. Finally a goal is to utilize measurement made on two variable speed turbines to compare the theoretically obtained results.

1.5 Thesis Layout

Chapter 2 presents an overview of the most important theories.

Chapter 3 describes the measurement equipment, hardware and software. Details about filter unit, sample and hold, card etc...

Chapter 4 Modelling of the most important part like: pitch actuator, spatial filter, rotational sampling filter.

Chapter 5 Proposals of different control schemes and tuning issues.

Chapter 6 Analysis of different control structures at different wind speed intervals.

Chapter 7 Control algorithms for whole wind speed region, switching methods between wind speed intervals and simulation result.

Chapter 8 Provides final conclusion and topics for future research.

Appendixes Measurement data from behavior of real wind turbines(Bast and Jung Turbine), Simulink implementation of the controllers, synthetic wind speed program listing in Matlab .

Chapter 2

Wind Turbine Operation

A wind turbine obtains its power input by converting some of the kinetic energy in the wind into a torque acting on the rotor blades (the actuator disc). The amount of energy which the wind transfers to the rotor depends on the wind speed, the rotor area, blade design (pitch angle) and the density of the air. Although there are many different configurations of wind turbines systems they all work in a similar way.

The turbine starts to produce energy when the wind speed is above V_{cut-in} and stops when the wind speed is below $V_{cut-off}$

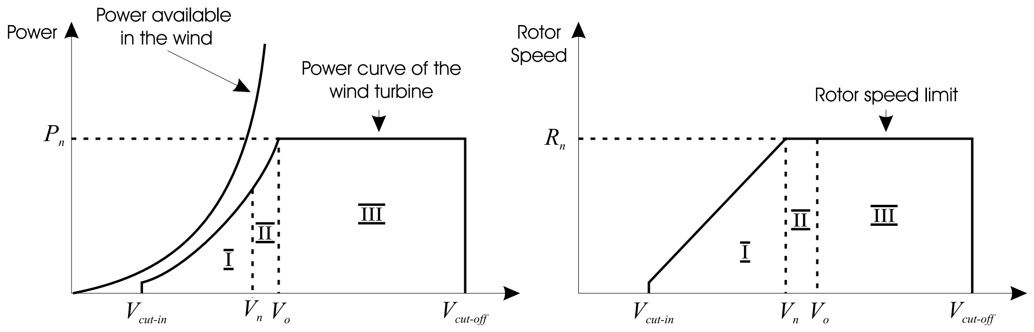

Figure 2.1. Different regions of wind turbine control

The control of a wind turbine consist three areas:

I. [V_{cut-in} ... V_n] Area where the turbine operate at "variable-speed" with an optimal rotor speed giving maximal energy.

II. [V_n ... V_o] Operation around rated rotor speed, but below rated power.

III. [V_o ... $V_{cut-off}$] Turbine operate at full power and rated speed, pitch control active.

2.1 Fixed and Variable Speed Operation

2.1.1 Constant Speed Operation

Due to its simplicity, the fixed speed turbines became the standard wind turbine for several decades. The fixed speed operation is obtained by directly connecting the induction generator stator's circuit to the grid. The rotor shaft is almost locked with the frequency of the electrical grid, admitting only a small (few %) variation from its nominal value. With constant speed the fluctuation of the wind speed will lead to fluctuating torque in the shaft which will result in fluctuating power, which might cause voltage fluctuations on a weak grid. The shaft torque pulsation will result in high stresses on the rotor, shaft, gearbox and generator. If we study the equation

$$P_a = \frac{\rho}{2}\pi R^2 C_p(\lambda) WS^3 \tag{2.1}$$

where ρ is the air density, we can see that there is no possibility to always operate the turbine with the maximum C_p efficiency in the whole wind speed range, because λ is inversely proportional to the wind speed

$$\lambda = \frac{\omega_r R}{WS} \tag{2.2}$$

that means the power coefficient is only optimal for a specific wind speed interval.

Another extra part is the capacitor bank typically designed to compensate for the induction generator no-load reactive power consumption also, a soft starter is a standard part of the fixed system. It is used only during the start up of the turbine and it lowers the current when the turbine is being connected to the grid. A wind turbine without a soft starter would draw a very high current during start up and the corresponding voltage drop in the grid would exceed the stated limits. Moreover, the gearbox would suffer from transient torques. Nowadays they become less economical because required heavy support structures to make safety above-rated wind speed due to high trust forces from the wind.

2.1.2 Variable Speed Operation

With variable rotor speed it is possible to operate at ideal λ, at maximum C_p value. It lead to extract maximum possible energy at the low wind speed range .This is important advantage of variable rotor speed. Today it can be obtained by using a power electronics converter. The types of generators used today are induction and synchronous machines.
Other important advantage it is reduction of drive-train mechanical stresses by better torque control which also result in better output power quality and reduced noise emission. Also smaller and cheaper gearboxes can be used due to the reduction of mechanical stresses. Today an aerodynamic power control principle (pitch control) almost exclusively is used in combination with the variable-speed turbines (see next section for explanation).

2.2 Aerodynamics methods for limiting the power

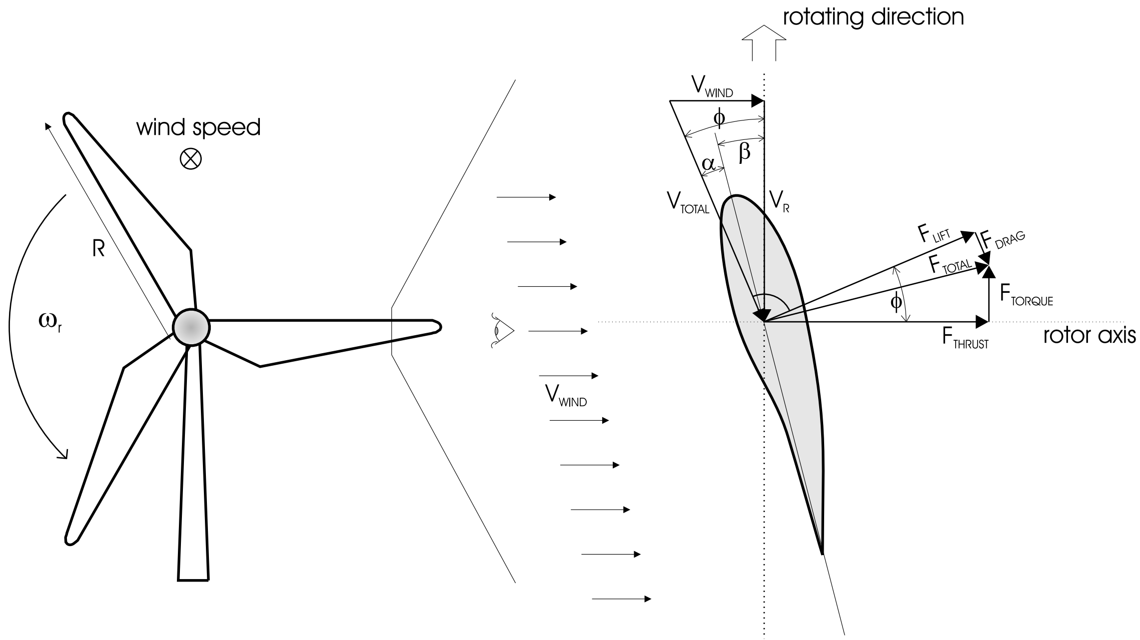

Figure 2.2. Aerodynamic forces and velocities at a rotor blade

There are two methods to limit the aerodynamic conversion at high wind speed. Pitch control which turn the blades out of the wind and stall control, where the blades loose their aerodynamic efficiency at high wind speeds. The amount of energy that is extracted from wind and converted into mechanical energy is depending on the radial force acting on the blade. The formation of the force depends on particular profile design and dimension and is shown in Figure 2.2. The $C_p(\lambda, \beta)l$ characteristic gives us a power coefficient, that depends on the tip speed ratio λ and the pitch angle β.For blade profiles two forces are generally used to describe the characteristics, lift force component (F_{LIFT}) and a drag component (F_{DRAG}) which resulting as F_{TOTAL}. The F_{LIFT} component and a F_{DRAG} together are transformed into a pair of axial F_{THRUST} force and rotor's directions F_{TORQUE} components, where only the F_{TORQUE} produces the driving torque around the rotor shaft. By varying the pitch angle, β the size the direction of F_{TOTAL} components can be changed. The axial forces F_{THRUST} has no driving effect but puts stress on rotor blades and furthermore, leads to a thrust on the nacelle and on tower.

2.2.1 Pitch Control

In this method there is a mechanism to physically turn the blades around their longitudinal axes. At low wind speed a control system will use this feature to maximize energy extracted from the wind. During the higher wind speed the

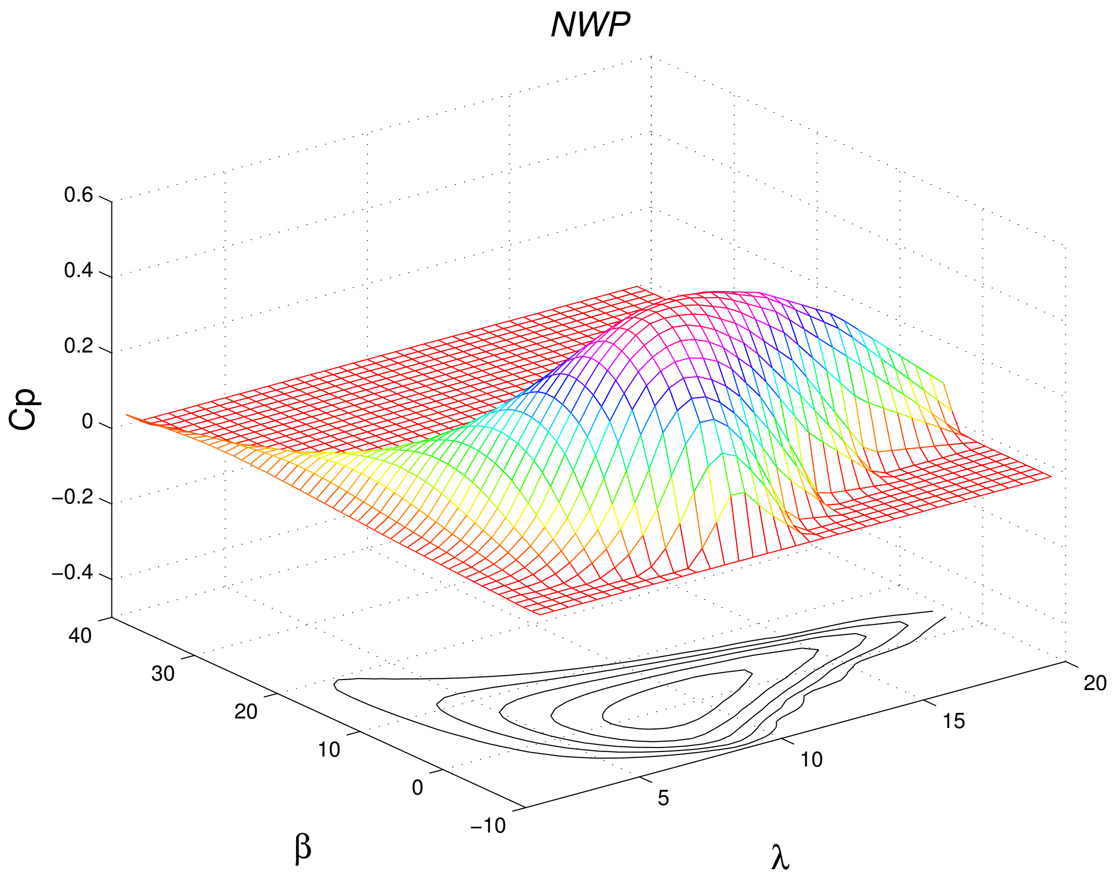

Figure 2.3. Calculated $C_p(\lambda, \beta)$ surface base on real data blade

torque or power can easily be limited to its rated value by adjusting the pitch angle β. In addition the axial aerodynamics forces are reduced. This method is almost always used with variable speed turbines in order to make operation at high wind speed possible and safety.

On a pitch controlled wind turbine the turbine´s electronic controller checks the power output of the turbine constantly. When the power output becomes too high, it requested the blade pitch mechanism to immediately turns the blades slightly out of the wind. When the wind speed is less strong the blades are turned back, into the most effective position.

2.2.2 Passive stall regulation

Passive stall controlled wind turbines have the rotor firmly attached to the hub at a fixed angle. Accordingly, using the passive stall method the pitch angle β is always constant, no mechanism to turn the blades around their axes is necessary. The blades are aerodynamically designed to stall at higher wind speeds, and the incoming power is limited close to the rated. When the wind speed increases, the angle α, which is the angle of attack, will increase. Above a certain angle α

the stall effect occur, the torque producing force can be limited approximately to its rated value. This concept is used for around 60% of the constant speed wind turbine in the world [www.windpower.org].

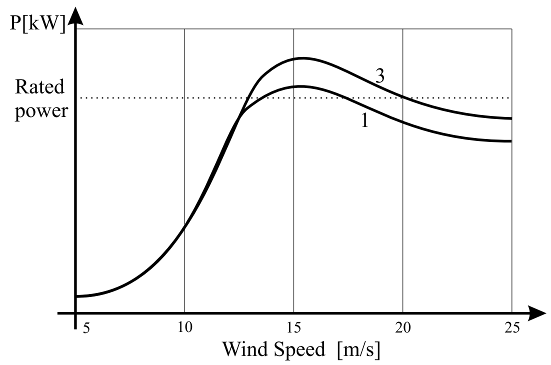

Figure 2.4. Effect for different pitch angles with constant speed operation

Advantages of the stall control system is that moving parts in the rotor blades are avoided and a complex control system is not necessary. On the other hand, stall control involves a very complex aerodynamic design and related design challenges in the structural dynamics of the whole wind turbine, for instance to avoid stall-induced vibrations. A normal passive stall controlled wind turbine usually have a drop in the electrical power output for higher wind speeds, as the rotor blades go into deeper stall, which is a drawback. For fixed-speed operation, an advantage is that stall-control gives lower power pulsation compared to pitch control [7]

2.2.3 Active stall regulation

The active stall regulation offers both, the advantages of pitch-controlled blades and the stall effect. Due to the pitch-controlled blades, one of the advantages of active stall is that one can control the power output more accurately than with passive stall, so that the average power is always at the rated value at wind speed above rated. As with pitch control it is largely an economic question whether it is worth to pay for the added complexity of the machine, when the blade pitch mechanism is added.

Besides providing power control, the blade pitch system is also used to accelerate the blades from idling to operational speed and bringing the rotor back to a safe idling situation in case of a grid loss or any other functional error.

The rotor blades are able to be pitched like the pitch controlled wind turbines. The difference is that when the machine reaches its rated power, the blades will pitch in the opposite direction, increasing their angle to the wind and going into a deeper stall.

The active stall control system is often installed in the large fixed speed turbines (1 MW and more).

Chapter 3

Data Collecting Equipment

3.1 Hardware

To collect data from the wind turbine site we need proper measurement and recording equipment which will be able to collect several channels with high sampling rate for many days. The range of power which will be measured is up to 850kW. Since the voltage level is 690V, the rated current is up to 600A. In order to measure the current we use LEM modules as current transducers. In order to measure the voltages we use an isolation amplifier and a resistive divider circuit. Also we have to chose the proper sampling frequency which allows us to reconstruct the shape of measured data in the future. Our data acquisition system is based on a PC computer with an installed data acquisition card. The DAQ card is connected to a filter box. The voltage signals from the current clamps and voltage probe unit feeds the filter unit with anti alias routines. The purpose of the voltage box is to reduce the measured voltages and obtain galvanic separations. The outputs signal level should match witch the range of the input voltage of the filter unit. The measurement set-up scheme is shown in Figure 3.1.

3.1.1 Measurement computer and surrounding

The computer is placed in an isolated place. Due to long distance to the wind turbine we would like to have some type of communication with the unit. Accordingly there is a GSM modem installed in the computer and proper software to operate the PC from a remote host which is located at the department. The modem unit consist of a modem and a GSM radio modul. We also equipped our unit with a UPS which is able to supply the computer for at least 10 min if there would be a black-out.

3.1.2 DAQ card

The most important part in whole system is data acquisition card. We have used a Microstar DAP 4000 card which occupies one PCI slot in the PC. This card is suitable for wide range of application in laboratories and industries.

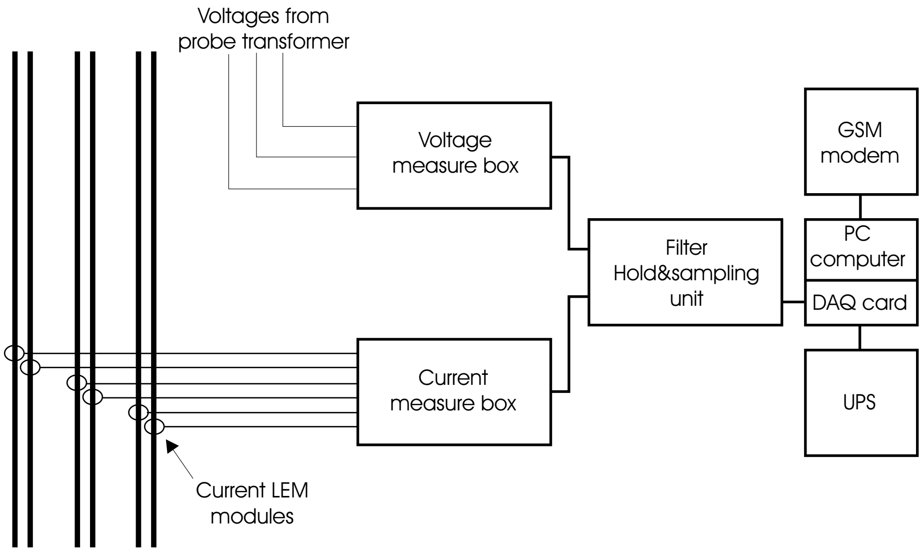

Figure 3.1. Overview of whole DAQ system

Figure 3.2. Whole measurement system

The DAP 4000 has a high performance Data Acquisition Processor for high speed data acquisition and control.

The main feature of the card are:

- TI 486 SXLC2-50 Processor
- PCI bus interface
- 14bit A/D converter resolution
- 800 thousands samples per second
- $\pm 2.5V$, $\pm 5V$, $0 - 5V$ and $0 - 10V$ analog input ranges

- Onboard operating system optimized for 32 bit operation

3.1.3 Filter and sample & hold unit

The filter unit with the sample and hold function included is set in 19" rack case. (Figure 3.3) There are 8 cards inside the unit, each consist two channels with differential voltages input.

Figure 3.3. Filter unit

The standard input circuit is shown in Figure 3.4. We are also able to adjust the gain of the input channels: $1V/V$, $2V/V$, $5V/V$, $10V/V$. In our case we set 6 channels to $\pm 2V$ sensitivity (gain: $5V/V$) to match the level with the output signal from the current clamps and the rest of voltage channels to $\pm 10V$. The

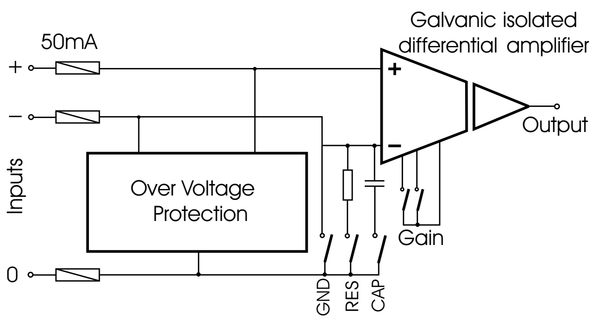

Figure 3.4. Input circuit with the galvanic operational amplifier

build in filter is a 4th order Bessel filter and the cut off frequency are: 10kHz, 2kHz, 416Hz, 104Hz and Bypass. We use this filter to avoid aliasing in case higher harmonics than relative present sampling frequency of DAQ card. In Figure 3.5 an overview of Sample and Hold unit is shown. Because it is not possible to measure two or more channels in one time without delay using the card only, we use a sample and hold unit to make simultaneous sampling possible. Usually this module is based on a multiplexed data acquisition card where many inputs are scanned by one A/D converter using a fast multiplexer. This module has to be synchronized with the DAQ card. It works like an analog memory, based on

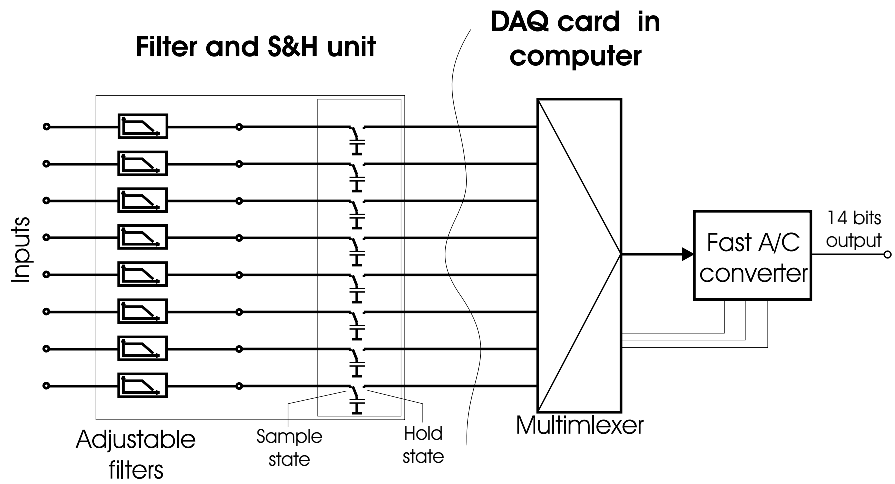

Figure 3.5. Principle of operation Sample and Hold module

capacitors. On the command by one synchronizing pulse all inputs are sampled and hold, and the measure process can be done. Now, the measured values taken at one time can be achieved by the multiplexer which have time to switch between the channels and there is no delay that can have influence on the final result.

3.1.4 Current Clamps

The current clamps (Figure 3.6) used in our project are operate using Hall-effect and they come from the LEM corporation. They are able to measure currents up to 2000A (peak) with an accuracy of 1%. The frequency range is specified from 0 to $10kHz$ within the -1dB bandwidth. The clamp ratio is specified as $1mV/A$ which give an output range $\pm 2V$ peak. That means that we can measure current up to 1410 A (rms value) and this is suitable for our purpose where the nominal current is around 600 A.

3.1.5 Voltage Probes

The voltage unit consist of galvanically isolated high accuracy operating amplifiers modules and a $\pm 15V$ power supply. On the high voltage side (the inputs) a traditional resistance voltage divider is used which adjust the level of the input voltages to values suitable for the DAC card. The galvanic separation assure us that there is no connection between computer and the grid in case of an error in the resistive divider. The resistors ratio is 1 : 20.1 and the max input voltage of DAC card is $\pm 10V$, $(7.07Vrms)$. So we are able to measure voltage up to 140 V

Figure 3.6. Current clamps with power supply unit(left), in real measurement (right)

with a 14 bit accuracy.
Resolution:

$$\frac{7.07 \cdot 20.1}{2^{14}} = \frac{142.12}{16384} = 8.675\left[\frac{mV}{step}\right]$$

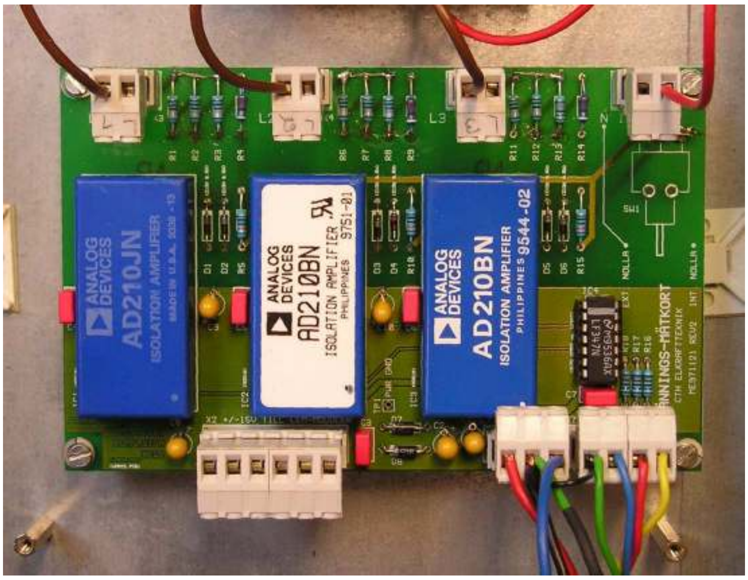

Figure 3.7. Galvanically isolated operating amplifier

3.2 Software and collected data

The program responsible for serving DAC card and store the data on the hard disk is DASY lab32. We have to decide what size of file we need and which track will be corresponding to which signal. To calculate the volume of data on HDD we have to know: sampling frequency, number of track, bytes per sample, time.

Example of calculating volume of data need:

$$2048[\frac{sample}{second}] \cdot 9[channels] \cdot 4[\frac{bytes}{samples}] \cdot \Big(60[sek] \cdot 60[min] \cdot 24[h] \cdot 7[days]\Big) = 42\frac{GBytes}{week}$$

3.2.1 File Data Format

There are many file format for data storage. Some standards are with header in the beginning of the file where we can found sampling frequency of the recorded data, sample format (float, double, integer, byte), triggering values, etc... The disadvantage of using that kind of format header is that we can not easily join files together or can not read sequently in the simple way.

Another group of format is without a header but in this case we have to known what kind of representation of data that has been used when acquire the file. The advantage is the simplicity of reading especially when we have large number of files.
For our purpose we have chosen the *IEEE* standard without the header, which is easy to read in Matlab. Each sample is described within 32 bites as a float number, and each file contains 16 channels of data. The length of the file depends on the number of samples. The data is organized in blocks, each block contains the sequence of the data samples (1,2,...,16) from one sample time and after there is another block corresponding to the next sample time.

Chapter 4

Modelling

4.1 Aerodynamic conversion - Spatial filtering

It is impossible to measure the "total" wind speed hitting the rotor, since the wind speed varies over the disc swept area. This gives us a problem since some of the control structures needs information about wind speed.
For the advanced modelling of the formation of the torque from the wind speed hitting the rotor disc (see Winkelaar [18]), the rotor area can be divided into rings and sectors, Figure 4.1, or also into cartesian coordinates. The wind speed at different points over the rotor swept area is then calculated. This approach gives a three dimensional wind speed map, across the rotor swept area. In this work only one dimensional wind speed signal will be used. In practise the calculation

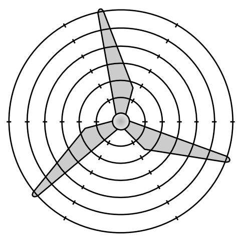

Figure 4.1. Rotor blades divided into sectors

of the aerodynamic conversion is usually obtain by using wind speed in one point. This one point wind speed is then made to represent an average speed over the swept area of the rotor, the rotor area itself acting as a low-pass filter using a transfer function

$$H_{SF}(s) = \frac{\sqrt{2} + bs}{(\sqrt{2} + bs\sqrt{a}) \cdot (1 + \frac{b}{\sqrt{2}} \cdot s)} \tag{4.1}$$

where $a = 0.55$, $b = \gamma \cdot R/U$, R [m] it the turbine radius, U [m/s] is the average wind speed at the hub height, and γ is the decay factor over the disc ($\gamma = 1.3$). The transfer function 4.1 can be simplified to a first order transfer function with a negligible effect on its characteristics.

$$H_{SF}(s) = \frac{1}{sb + 1} = \frac{1}{\frac{s}{2\pi f_{cut}} + 1} \tag{4.2}$$

where f_{cut} [Hz] is the cut-off frequency of the filter. The outgoing signal from filter is the equivalent wind speed representing the average impact of the wind field experienced by rotor. The comparison between one point measured data and with filtered data is shown in Figure 4.2 and Figure 4.3

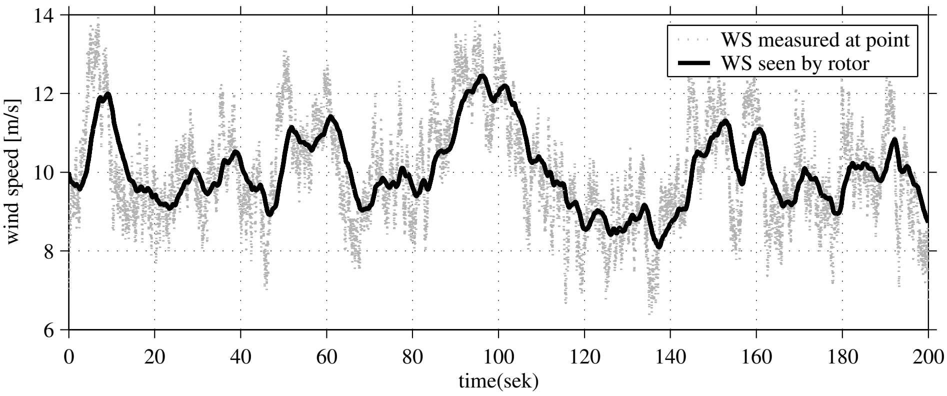

Figure 4.2. Filtering property of the rotor blades

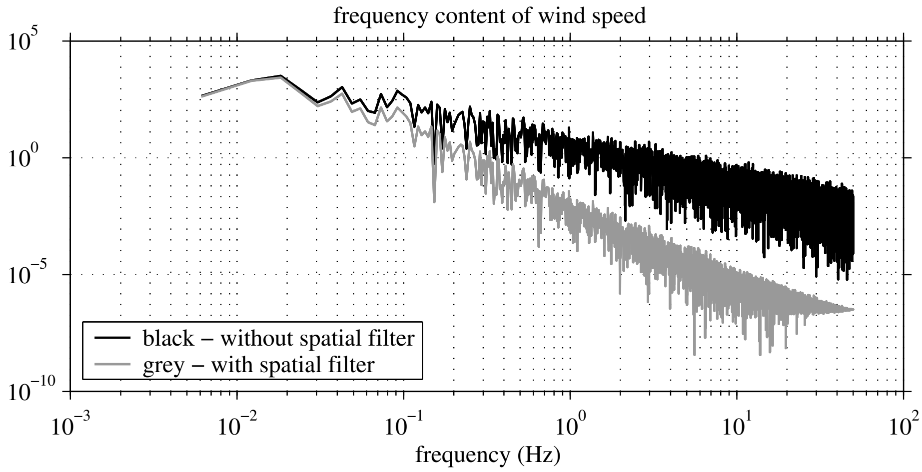

Figure 4.3. Influence of the spatial filter for frequency spectrum

4.2 Rotational Sampling Filter

According, to [1] improve the validity of the actuator disc model we apply a filter called rotational sampling filter. This filter amplifies the variations at a frequency region around the blade passing frequency. In other regions, this filter has a gain of nearly one. Especially in middle wind speed region this effect it will provide some disturbance and special attention has to be made in the controller design.

[1] In reality, there will be areas swept by the rotor blades that has higher wind speed than other, this will lead to that the torque will consist of a pulsating component at the same frequency as the blades pass this area

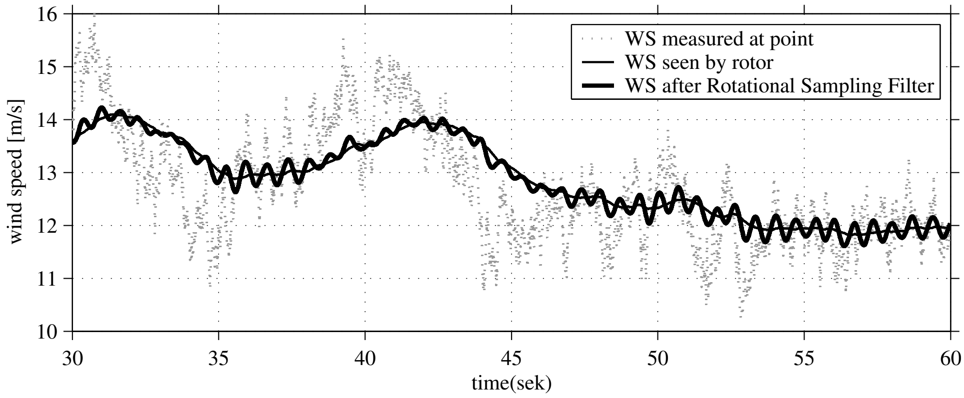

Figure 4.4. Wind speed measured at one point and filtered with spatial filter and RSFilter

The transfer function of this filter is:

$$H_{RSF}(s) = \frac{\frac{1}{\omega^2}(s+\omega)^2}{\frac{1}{(\omega^2+d^2)}[s+(d+j\omega)][s+(d-j\omega)]} \tag{4.3}$$

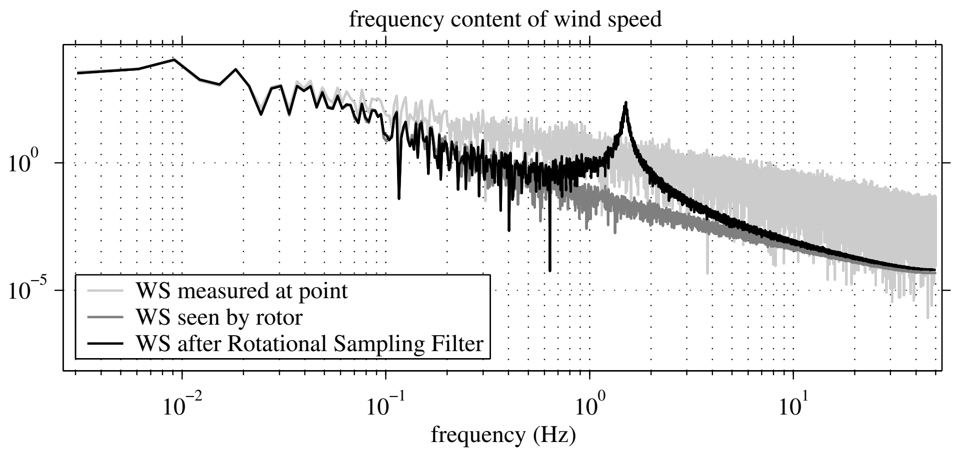

Figure 4.5. Influence of the RSFilter for frequency spectrum

4.3 Modelling of Pitch Actuator System

Blade pitch control is primarily used to limit the aerodynamic power above rated wind speed in order to keep the turbine shaft torque within its design limits.The inertia of the blades turned by the drive is large and the pitch actuator has thus limited capabilities. Its dynamics are non-linear with saturation limits on pitch angle (usually from $-3°$ to $90°$) and pitching speed rate (around $8°/sec \div 10°/sec$).

In this work, two pitch angle control structures are evaluated

- as integrator with prevented 'winding up' and saturation range.

- as on-off model with three levels of speed using an integrator.

4.3.1 Pitch Actuator as Integrator with Saturation

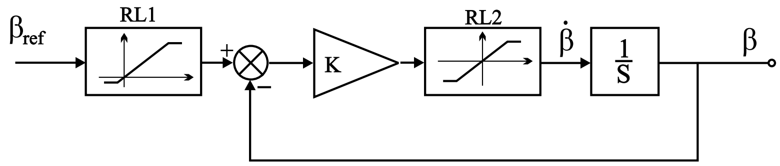

Figure 4.6. Pitch actuator I

The simplest model of the the pitch-actuator proposal is shown in Figure 4.6, where:
$RL1$ is the pitch angle limitation,
$RL2$ is the pitching speed limitation
K is the 'softness' coefficient when the limit is approaching.

This actuator is modelled in closed loop with saturation of the pitch angle and a pitch rate limitation. In this closed loop configuration with integrator, its gives similar result as a first order transfer function but with limitation of the pitch rate. Also while the β_{ref} is on the lower limit, the integrator is prevented from growing indefinitely or winding up.

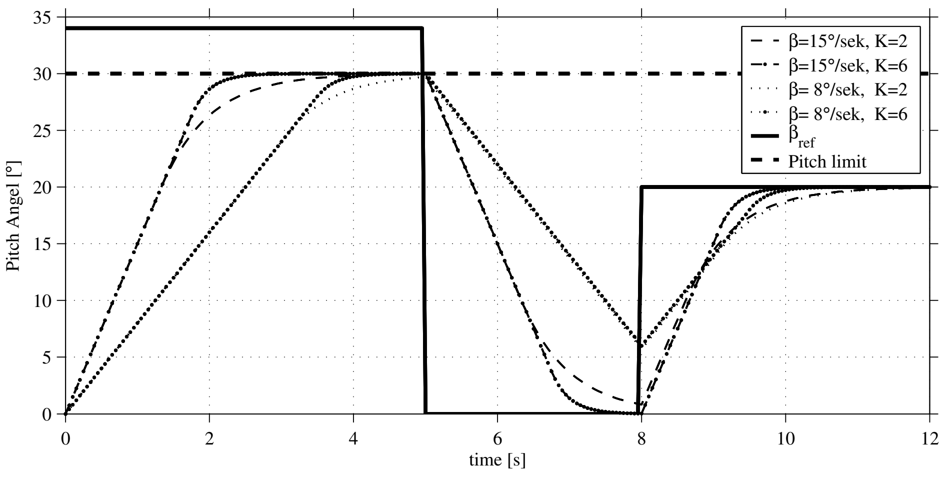

Figure 4.7. Responses of pitch angel demand

In Figure 4.7, step responses for two different ramping speeds and two different K coefficient are shown. The solid line represents the reference value and the thick dashed line the used pitch angle limitation.

4.3.2 Pitch Actuator with Three Levels of Pitching Speed

This actuator is modelled as a three pitching speed actuator. It can perform the pitching only with one fixed speed in both directions or it can remain at a constant angle. So if the signal error is greater than the trigger level, a pitch acting with a constant speed is ordered until then error signal become lower than the trigger value. When this happens the pitching stops and the angle remains in one position. The error signal comes from the controller and is usually based on the power error. The block scheme is shown in Figure 4.8. This approach

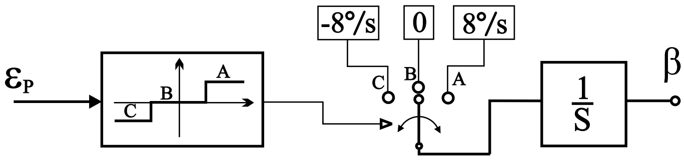

Figure 4.8. Pitch actuator II

of actuator is slightly different than the previous one since the information for input is based on error not in a certain value. The pitching is only active when the error level is outside the dead zone values, otherwise the pitching mechanism remain at rest. This behavior is better from a practical point of view because it needs much less pitch activity and is more ”structure friendly” due to that pitch actuator will be at standstill for longer period of time. So the pitching is not performed constantly like in the first pitch actuator proposal.
The step performance with different ramp settings are shown in Figure 4.9

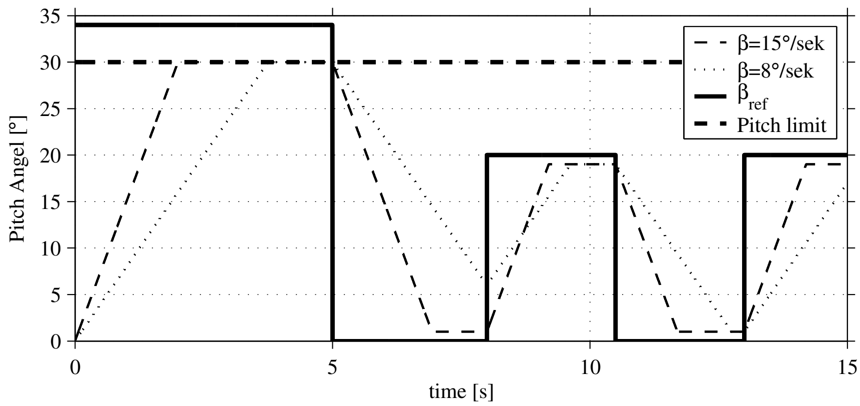

Figure 4.9. Step Responses

As we can see in Figure 4.9 the dead zone is set to ±1 and can be easily adjusted to fit with controller.

4.3.3 Summary of the Pitch Actuators

In Figure 4.10 a comparison of both pitch actuators approach done with these same condition is shown.

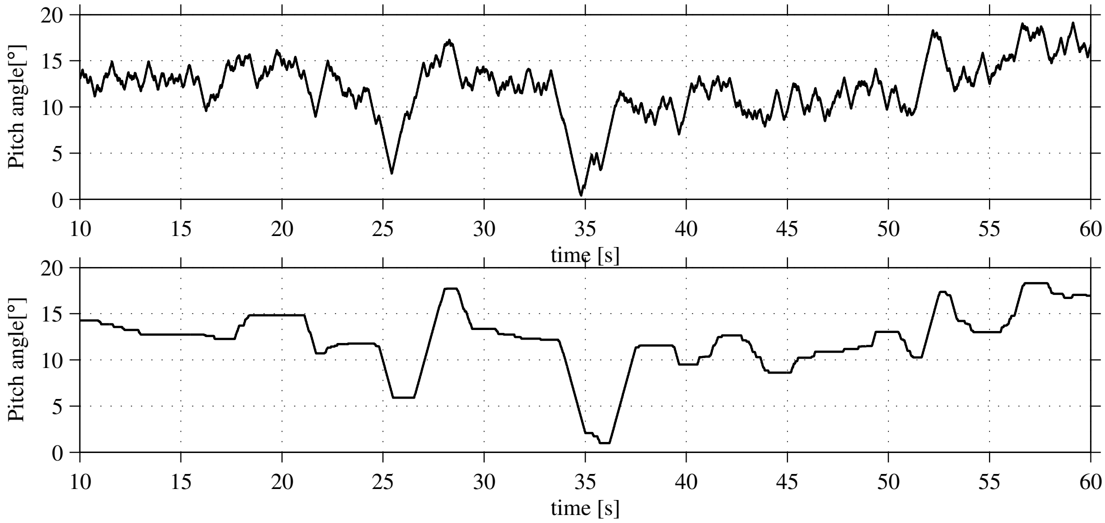

Figure 4.10. Comparison of two pitch actuators activity

Pitch actuator	active time[%]	number of switching
with integrator	100 %	208
3 speed level	26%	66

In the Figure 4.10, in the upper diagram a pitch activity with the version of actuator using integration and the lower one shows the method of using three levels of speed is shown. By adjusting the dead zone we can make a more 'sharp' or 'flat' behavior and it is insensitive from a controller gain tuning point of view. In this simulation the controller parameters in both cases were tuned to get the same power deviation and make the both pitch actuators structures comparable. The first approach is very sensitive to controller gain tuning and hence the activity of pitch is continuous, as can be observed from the figure, which will wear out the mechanism unnecessarily.

In the following, the three speed level actuator will be used as it seems to be a better choice. The main disadvantage of the first version actuator is that we cannot predict which β angle we will needed at that time when the actuator has reached command value. At this time the wind condition may have changed and then we will need another setting. The second version compare 'on line' the proper criterium and then decide, if to increase or decrease the pitch angle, without predicting the future angle like in the first version.

Chapter 5

Controllers

5.1 Different Control Needs for Different Wind Speed Interval

the whole operating range for a variable speed wind turbine has been in this work divided into three different control regions corresponding to three different wind speed intervals. In each of them, the reference or tracking value of the controller is different, depending on the interval. Below rated power, in low wind speed operation we try to get as much energy as possible from wind. This region usually starts from 4m/s and ends around to 9-10 m/s when the maximum rotor speed is reached. Usually this is control by trying to track the top of the $C_p(\lambda, \beta)$ efficiency surface where the efficiency is as greatest.
In the middle step interval the controller usually keeps the speed at nominal rotor value, and accordingly, the power gain cannot be kept at maximum efficiency.
The last interval begins when we reach nominal generated power and in this region pith control adjust the aerodynamical power to be at or below rated. This interval is valid up to around 25m/s where due to safety reason the turbine is disconnected and shut down.
These cases will be studied separately to get a proper behavior of each of the control strategies.

5.2 Low Wind Speed Operation

In this region there is a speed controller which follow the reference speed. According to equation 5.1

$$\lambda = \frac{\omega_r \cdot R_{blad}}{WS} \tag{5.1}$$

and information from the C_p efficiency surface, that only for one λ point we have the best efficiency for given pitch angle. From 5.1 we now have equation 5.2.

$$\omega_{ref} = \frac{\lambda_{max} \cdot WS_{SF}}{R_{blade}} \tag{5.2}$$

Where WS_{SF} is the wind speed seen by the rotor, and λ_{max} is the value that together with $\beta = 1$ gives the highest efficiency from C_p table. The control scheme is shown in Figure 5.1 The information about wind speed in most cases is

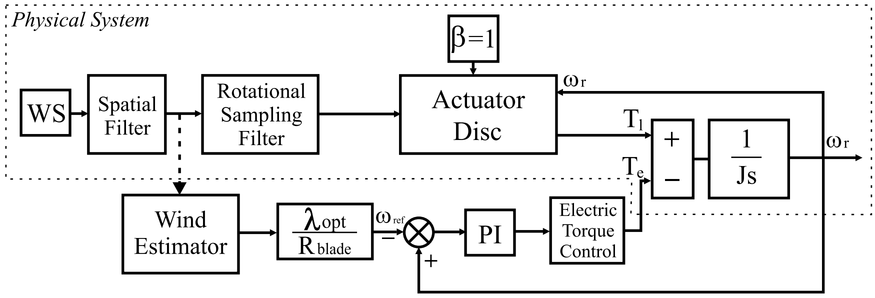

Figure 5.1. Control scheme in low wind speed

based on measurement and it's used to calculate the most effective rotor speed. The electrical torque demand is set by a circuit with a PI controller which has as input the difference between the actual and the most efficient rotor speed. By proper tuning of the PI controller there is a possibility to adjust the bandwidth of the speed control loop which have a large influence on the torque variation and the energy gain.

5.2.1 Controller Tuning

Applying only the proportional term in the controller, gives the result shown in Figure 5.2. In the figure, there are two different proportional gain settings of the controller. As we can see the higher gain gives a better following of the speed reference but to the cost of a more fluctuating torque. To calculate the K_p in steady state we have

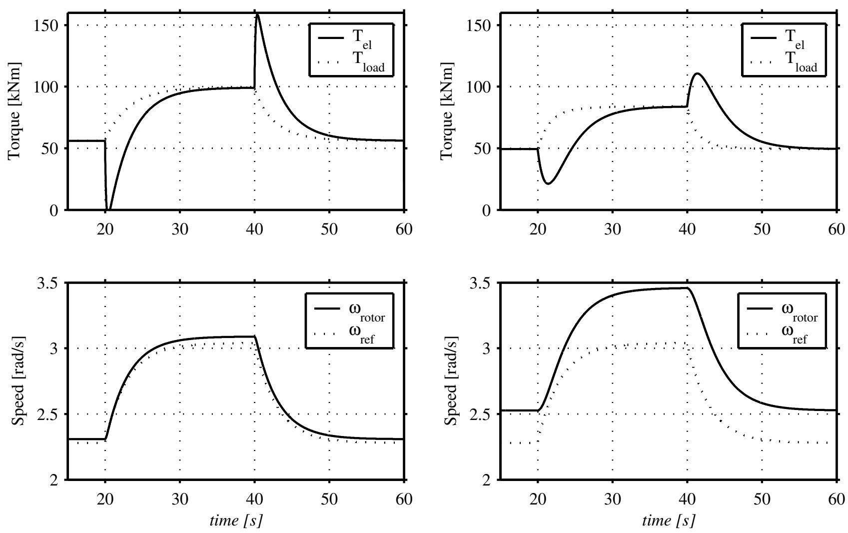

Figure 5.2. P=20 000 (left), P=2 000 (right)

$$K_p = \frac{T_{N_{el}}}{\Delta\omega} = \frac{T_{N_{el}}}{\omega_r - \omega_{ref}} \tag{5.3}$$

where $T_{N_{el}}$ is the nominal generator toque.

Full PI controller

If we consider to apply the integral part in the controller the offset can be cancelled as shown in Figure 5.3. Too high integral part may lead to that the system become unstable, or at least oscillatory.

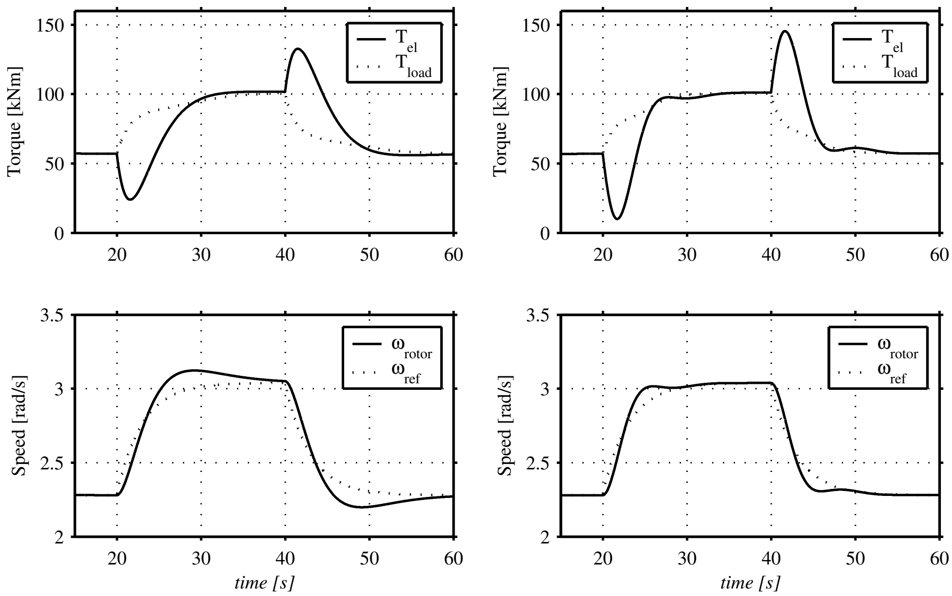

Figure 5.3. P=2000, I=500 (left), P=2000, I=2000 (right)

5.2.2 Step Response with Different PI Settings

The step response is studied using different controller setting. The wind is changed from 6 m/s to 8 m/s, the electrical torque is held in operating region of the generator. The result with "fast" (left) and "slow" (right) response settings is shown in Figure 5.4. As can be seen, the time responses for the speed and torque are very long, several seconds. Increasing the integral part has no great effect on the speed of the regulation, instead the fast response is determined by the proportional part.

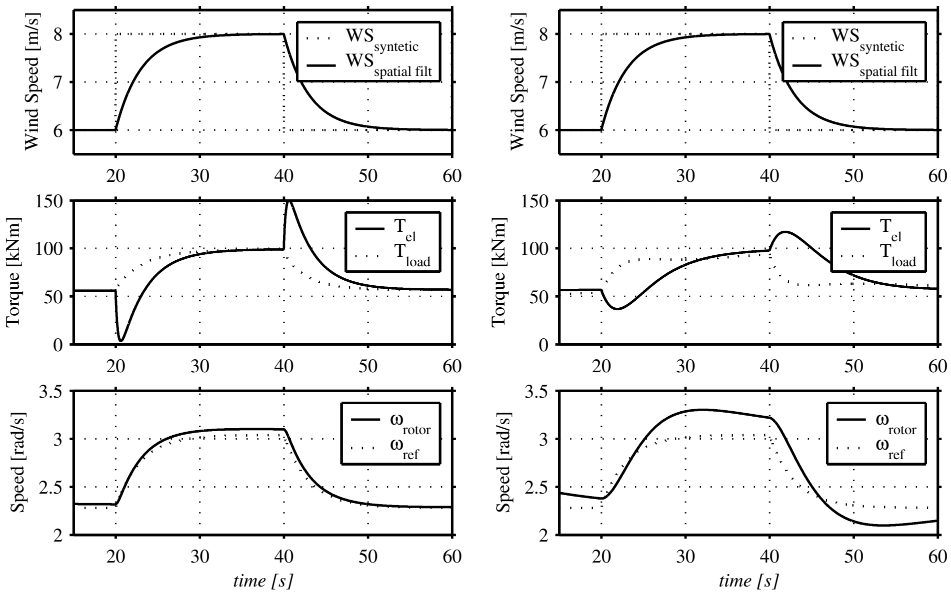

Figure 5.4. P=10e3, I=200 (left), P=1000, I=100 (right)

5.3 Middle Wind Speed Operation

In the middle speed operation we are trying to keep the rotor speed in a certain spam, described as a speed band around the maximum rotor speed. The rotor speed, torque and energy capture are determined similarly as in the case of a classic fixed speed wind turbine approach. Usually this interval starts at 9 m/s and ends when nominal generator power is reach (11-12 m/s) so in this region turbine operate below rated power. The basic scheme is shown in Figure 5.5 The

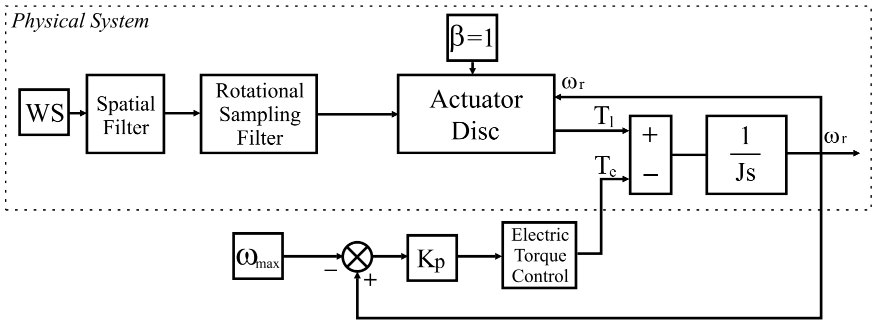

Figure 5.5. Scheme of rated rotor speed control

principle of regulator tuning, based on Equation 5.4.

$$K_p = \frac{T_N}{\sigma\omega \cdot \omega_{max}} = \frac{T_N}{\delta\omega_{max}} \tag{5.4}$$

where $\sigma\omega$ is the slip given in [%/100]
The example with slip=2.5% and 7.5% is shown in Figure 5.6.

The rated generator torque $T_N = 300$kNm.
Ac can be see in Figure 5.6 there is a offset dependent on the K_p gain. By

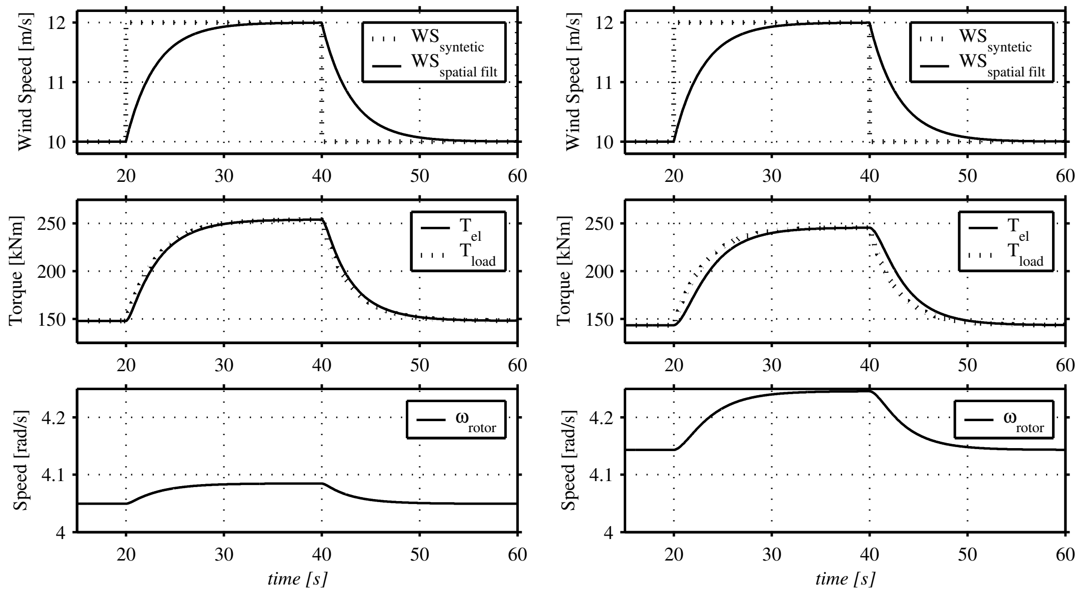

Figure 5.6. Different Proportional Part setting

introducing the Integral part in the control loop we can cancel this offset. The example with different integral and proportional part settings is shown in Figure 5.7.
As the generator speed is almost locked to the nominal, the variations in the electrical torque are directly responding to the loading torque generated by the incoming wind. This will apply that λ now is not fixed to the optimal value and the efficiency of the turbine is now directly determined by the C_p surface.

Since the rotational sampling filter is implemented in the model, the torque variations are higher than without implementation.

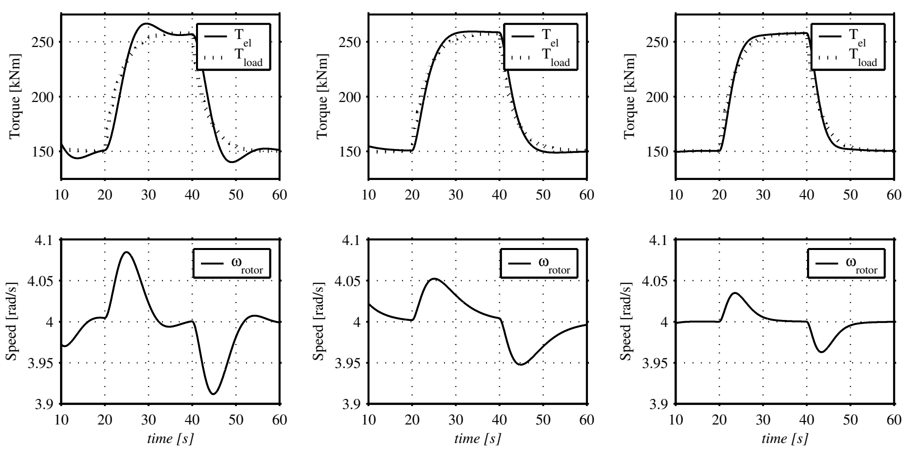

Figure 5.7. P=4000, I=2000 (left), P=10e3, I=2000 (middle), P=10e3, I=5000 (right)

Anti-rotational sampling filter

To avoid the influence from the rotational sampling for the controller we use low pass filter in the control loop. We can decrease the components above 0.6Hz where usually the components from RSF occur. The scheme with applied LPF and HPF is shown in Figure 5.8.

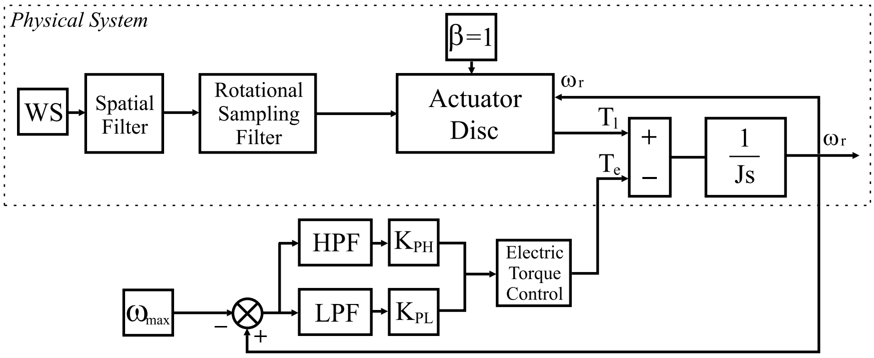

Figure 5.8. Control scheme of middle wind speed with additional filters

The LPF filter is to dump oscillations which may occur in ω_r as a result of rotational sampling. Moreover it improve torque demand quality as can be seen in Figure 5.9 right. The K_{HP} gain of the HPF is about 1/10th of the K_{LP} gain. The cut-off frequency is set to 0.6 Hz as proper in most cases. As we can see in Figure 5.9, right picture that with filter we get a more smooth torque than without a filter. By using that filter, decrease output power variation will follow.

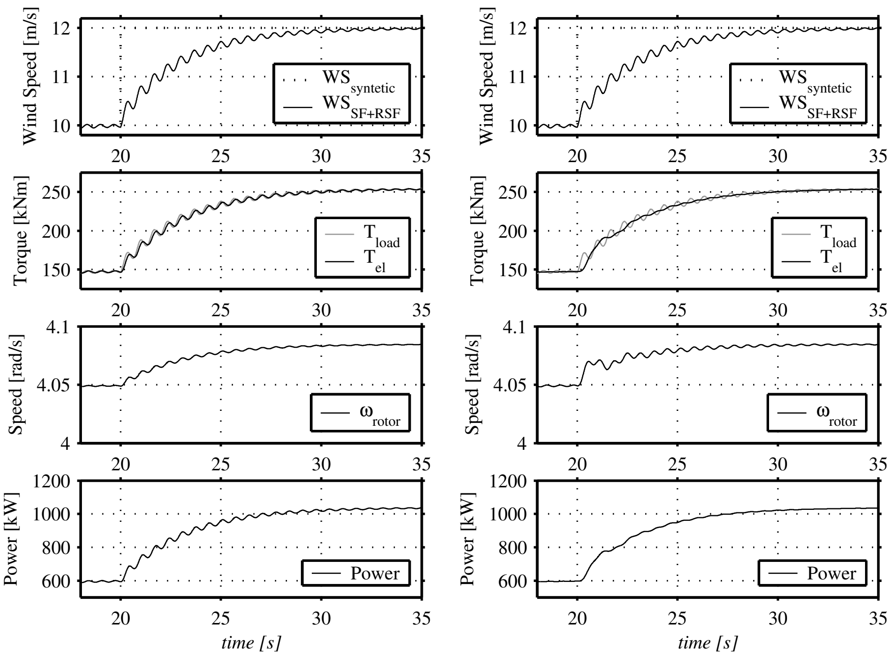

Figure 5.9. Differences with (left) and without (right) applying the extra filter

5.4 High Wind Speed Operation

In the high wind speed area the desired operation is to keep the rotor speed and especially the generated power as close as possible to the nominal. To reduce the surplus energy we using the blades pitching as a main power control in this region. The overview of the scheme is shown in Figure 5.10.

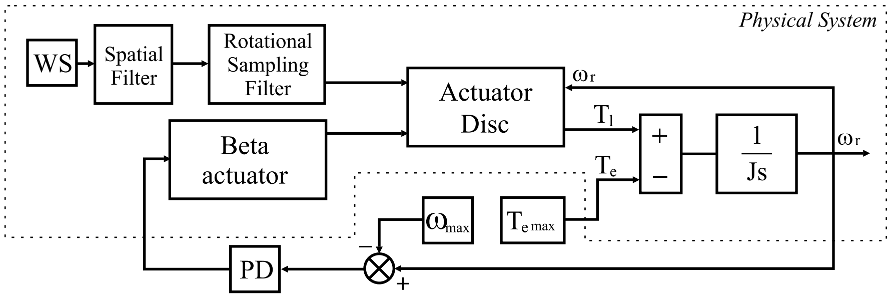

Figure 5.10. Pitch control scheme in high wind speed interval

The most crucial factor for the regulation is the possibility to quickly respond to variations in the torque generated by the wind which are detected by speed changes. This puts very high demands especially on the pitch actuator which tunes the blades to the desired position. In practise all pitch actuators has limited ability to fast change the angle of the rotor blades.

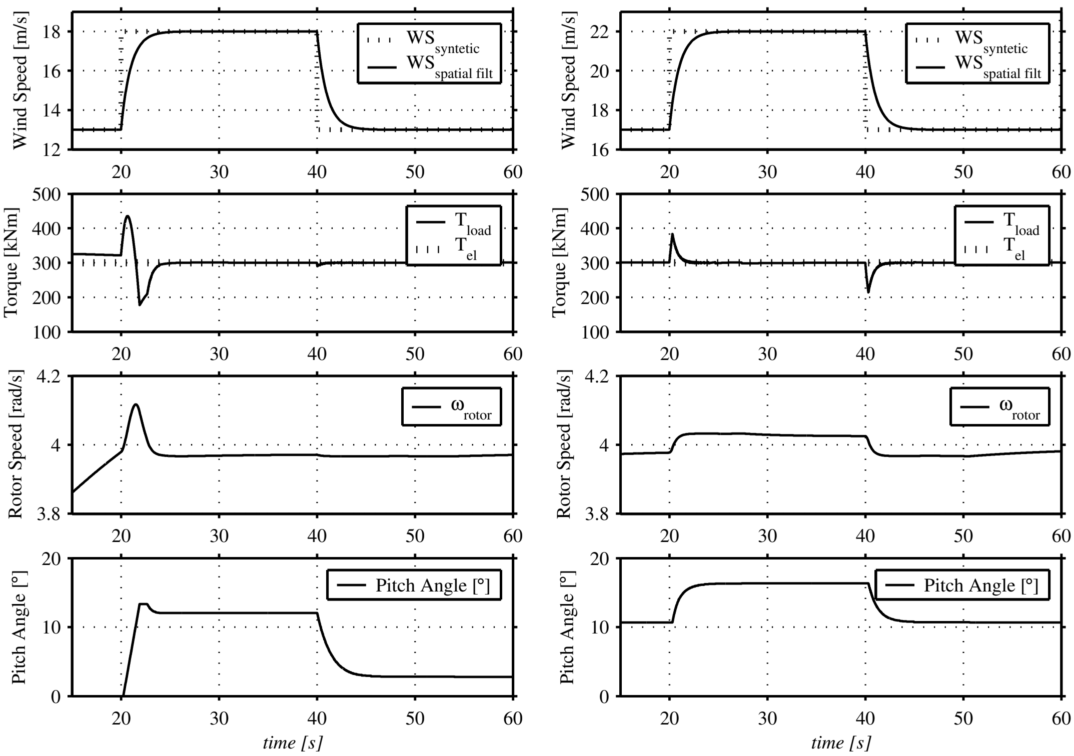

Figure 5.11. Pitch control responses for different wind speed steps

In the left and right part of the Figure 5.11 we see the responses of the pitch actuators using different wind speed steps. In the left picture the wind speed steps is from 13m/s to 18m/s and 17m/s to 22m/s on the right respectively. In the left picture, the pitch angle response increasing with maximum pitching speed which may mean that on the top of $C_p(lambda, \beta)$ surface is local equality and in order to decrease the C_p value the pitch angle, β must go further. When we have situation from right picture, we are already in proper operating area, and even small changing pitch angle lead to significantly change the C_p value.

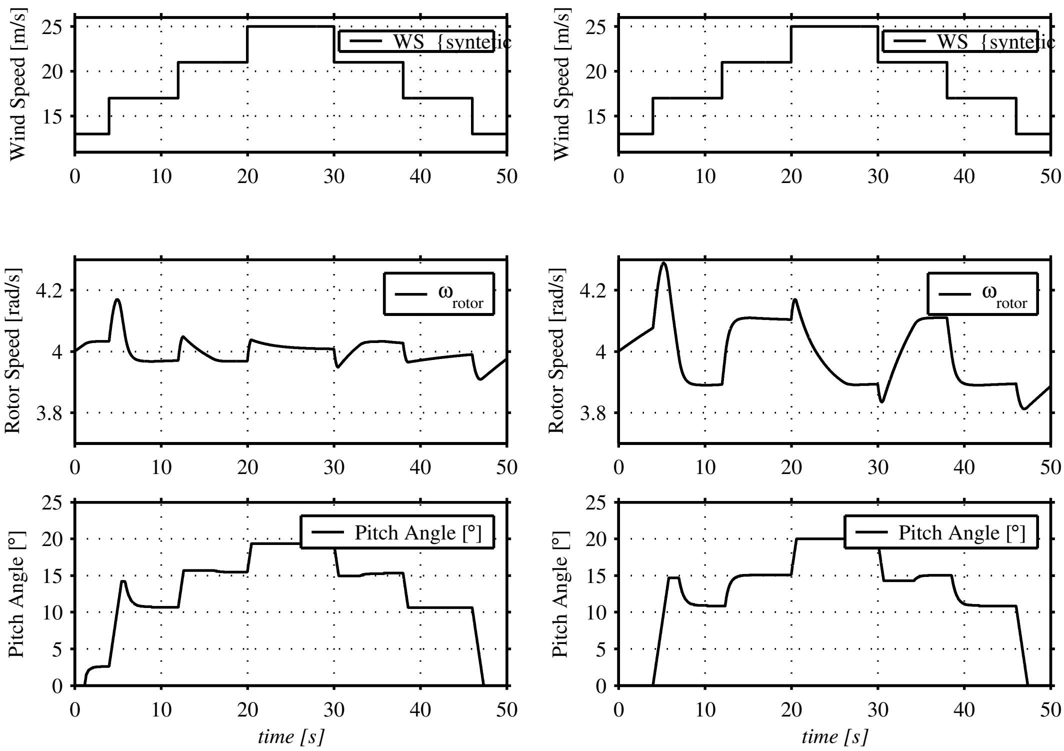

Figure 5.12. Pitch response with different control settings P=30, D=15 (left) P=9, D=5 (right)

In Figure 5.12 there are pitch responses and rotor speed with different PD controller settings. As we can observe the proportional part is responsible for correcting the pitch where the input is based on very slow varying signal. The good improvement is to introduce derivative part which is especially sensitive for fast changing signal which speed up pitching the blades. By keeping a proper proportion between the proportional part and derivative of the controller, the pitch angle behavior in both cases is similar but the rotor speed has different variations.

Changing the Derivation Part

There are three responses in Figure 5.13 with different derivation part setting in the controller. As we can observed this part helps in speeding up the pitching actuator action. It is sensitive for the fast changing signal of the input and sometimes overshoots can occur when the D part is too high.

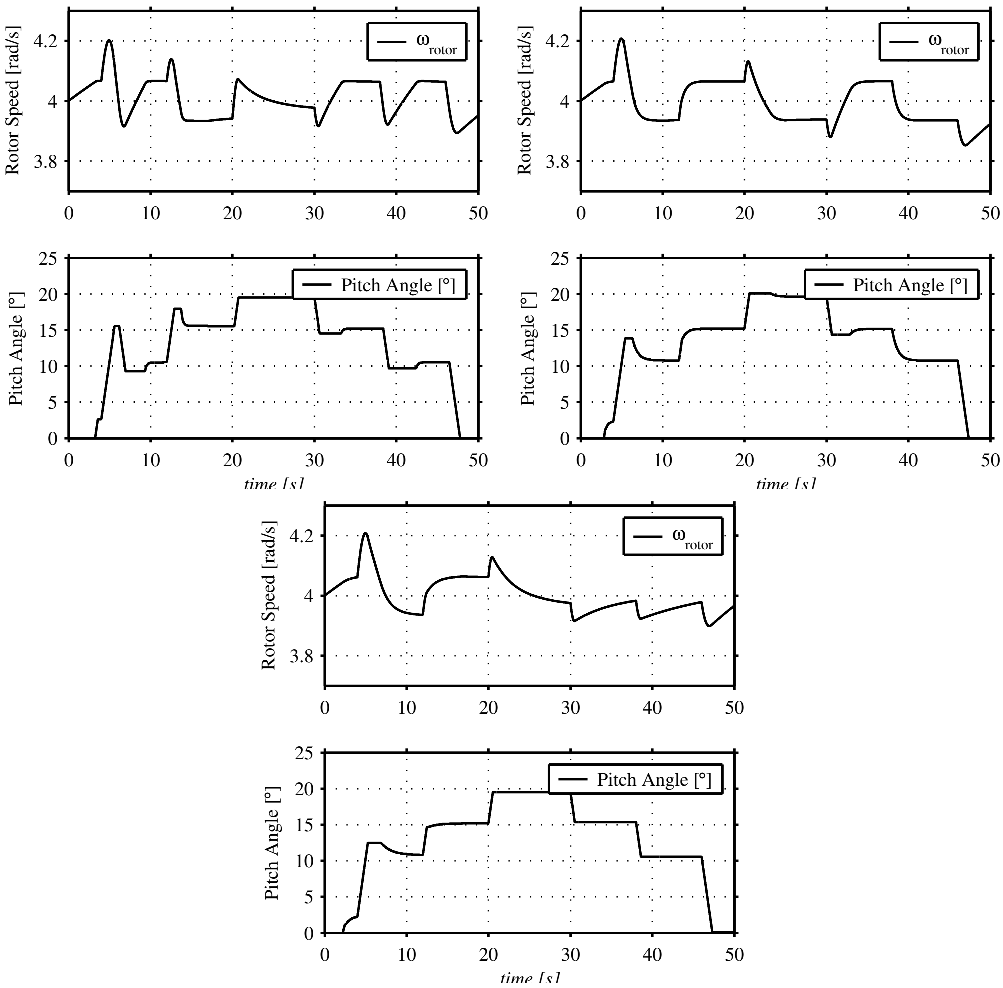

Figure 5.13. Pitch control responses P=10, D=2 (left), P=10, D=6 (right), P=10, D=12 (down)

Chapter 6

Analysis

In this chapter results of simulations in three different wind speed intervals will be shown and discussed.

6.1 Low Wind Speed Interval

In Figure 6.1 we expose our control system to real wind speed data. The wind speed series are shown in the top. The black line represents signal after spatial filtering which is given to a controller. The gray plot represents the actual wind speed.

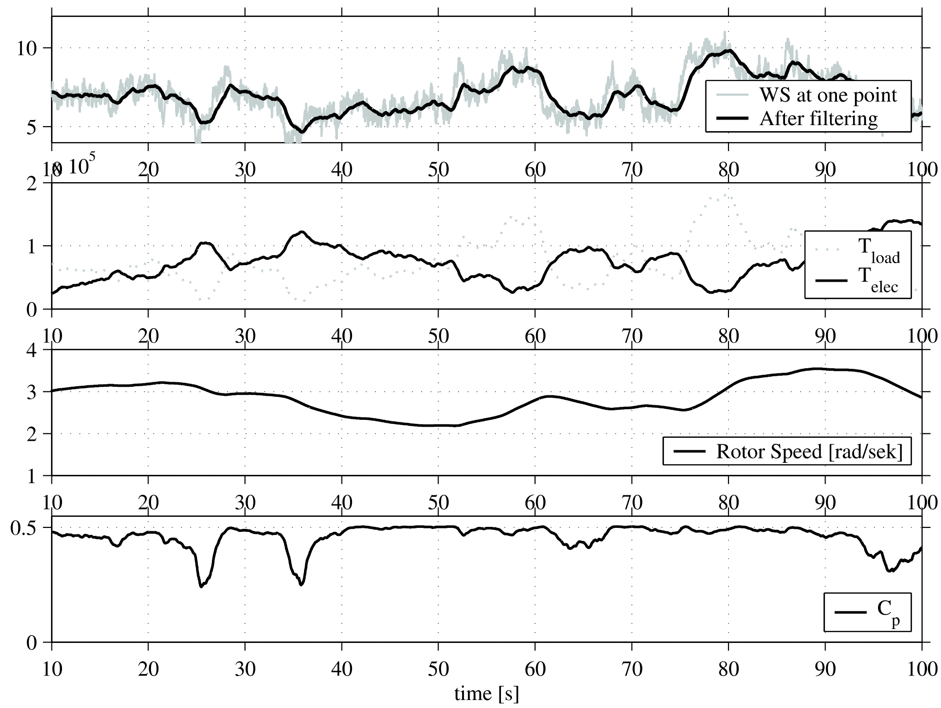

Figure 6.1: Low Wind Speed result diagram

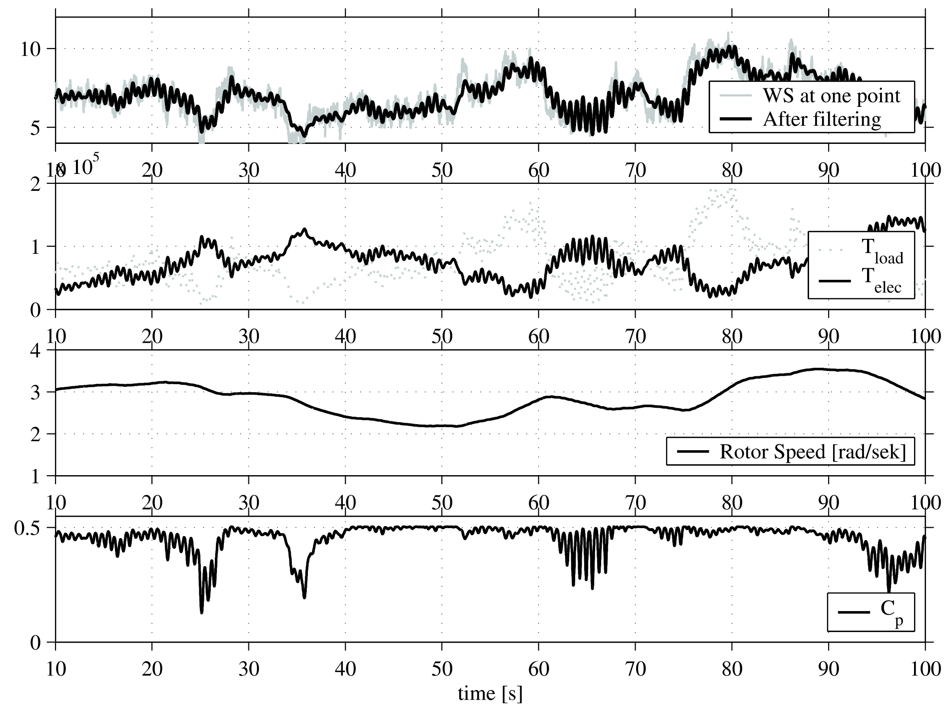

Figure 6.2: Low Wind Speed control result with applied RSF

Here we can see that the speed is tracking the reference speed very well and thereby keeping a good efficiency for the turbine's energy capture. On the other hand the fast tracking reference rotor speed may cause high torque variation.

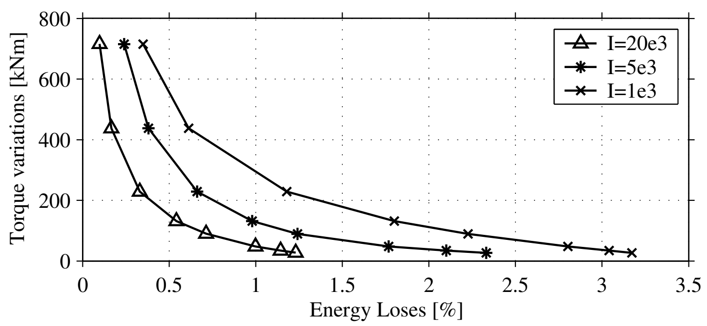

Figure 6.3. Standard Deviation on Torque Variation versa Energy Loses with RS Filter

There are three series with different integral part of the controllers setting showning torque fluctuations versa energy loses in Figure 6.3 and 6.4. The proportional part were a series with different gain $P = 1e3$, $5e3$, $10e3$, $20e3$, $50e3$, $100e3$, $200e3$, $500e3$.

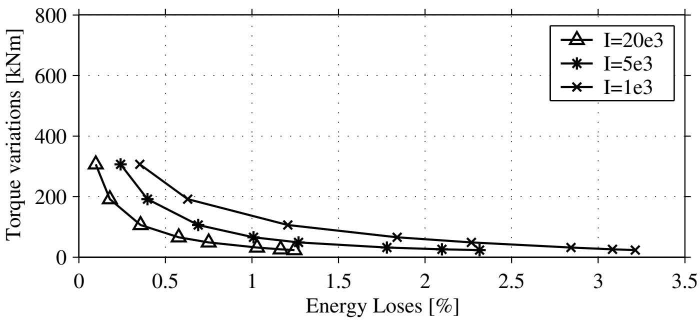

Figure 6.4. Standard Deviation on Torque Variation versa Energy Loses without RS Filter

As we can see on Figure 6.3 and 6.4 there is a big difference in torque variation after including to the model the rotational sampling effect which is caused by blade-tower passing frequency.

In Figures 6.5 simulating result using feed-forward structure proposed by Bossanyi [2] are presented.

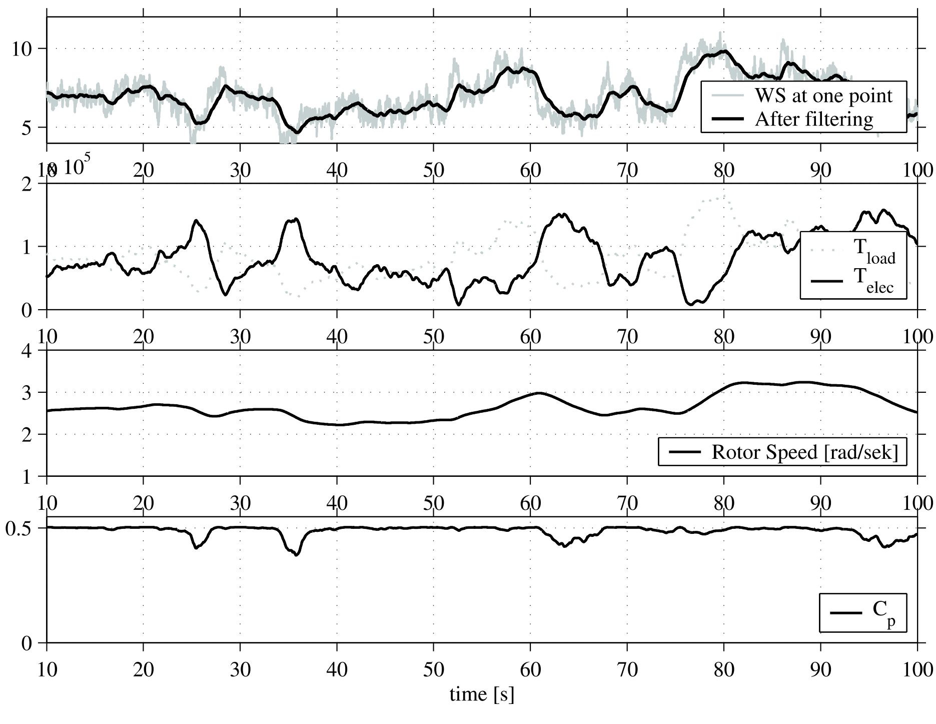

Figure 6.5. Low Wind Speed controller result

As we can see there is no big difference between the proposed control scheme and the one slightly modified by Bossanyi [2]. There is only a small difference in the rotor speed variation, which has an influence on the energy gain.

6.2 Middle Wind Speed Interval

The first plot in Figure 6.6 shows the wind speed before and after applying rotational sampling filter. The second plot in Figure 6.6 shows the electrical torque and the torque from the wind where they are almost the same in order to keep constant speed.

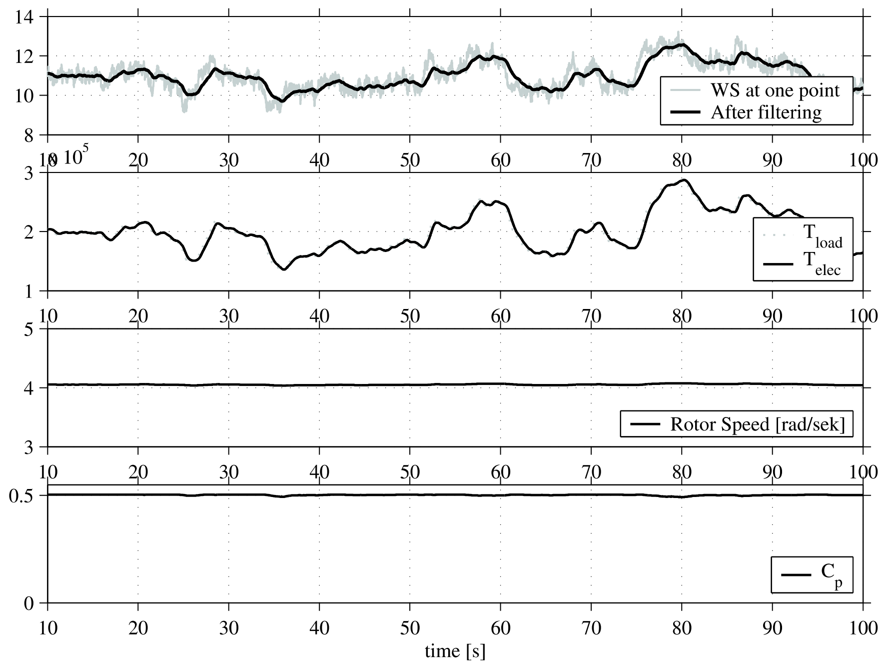

Figure 6.6. Middle Wind Speed Controller result

To obtain influence of maximal rotor variation on torque fluctuation, there 5 calculations have been done, for 1%, 2%, 5%, 10%, 20% of the rotor slip. The stresses of interest are the high-frequency component of the electrical component, therefore all simulations are high pass filtered with Butterworth filter. The standard deviation are presented in Figure 6.7.

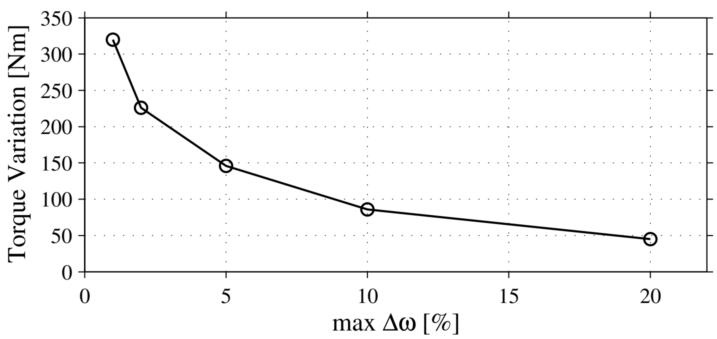

Figure 6.7. Torque variation versa maximal slip

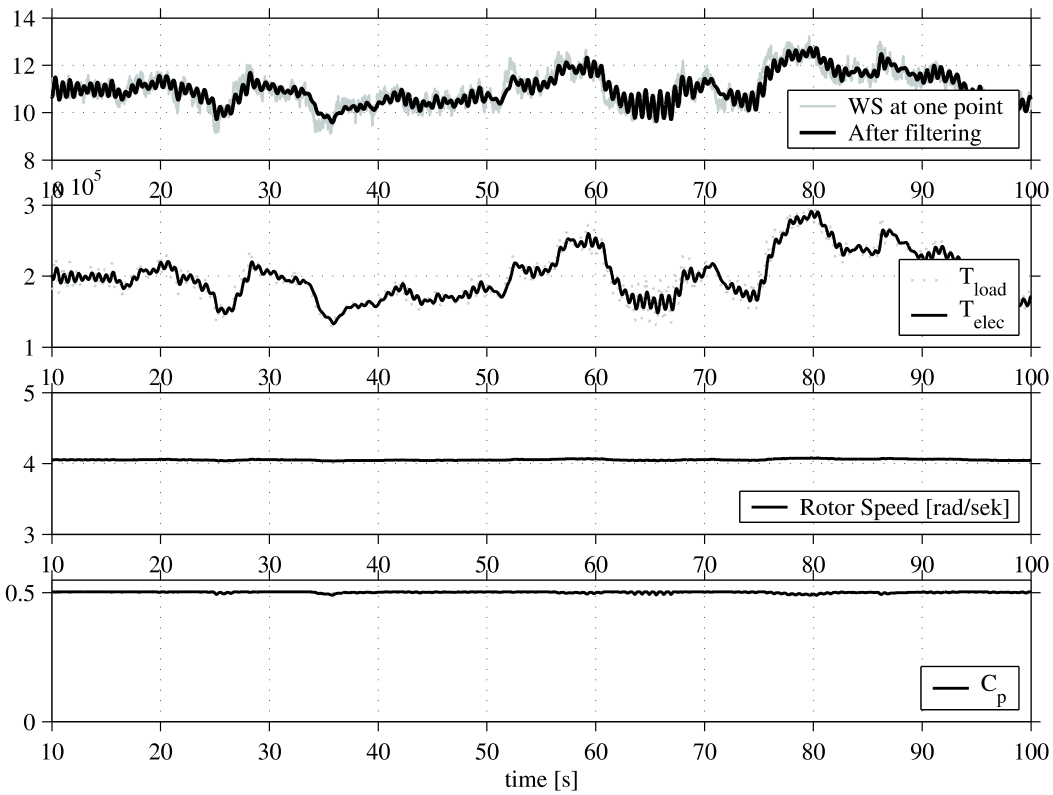

Figure 6.8. Middle Wind Speed Controller Result With RSF

The goal here is to keep the electrical torque and as well the rotor speed with minimal pulsation from influence of rotational sampling effect. As we can see in Figure 6.8 the rotor speed is prevented from pulsation with good result. The electric torque has some fluctuation, but they are easy to remove by using anti rotational sampling filter what is shown in Figure 5.9 and furthermore the output power is also without fluctuations.

6.3 High Wind Speed Interval

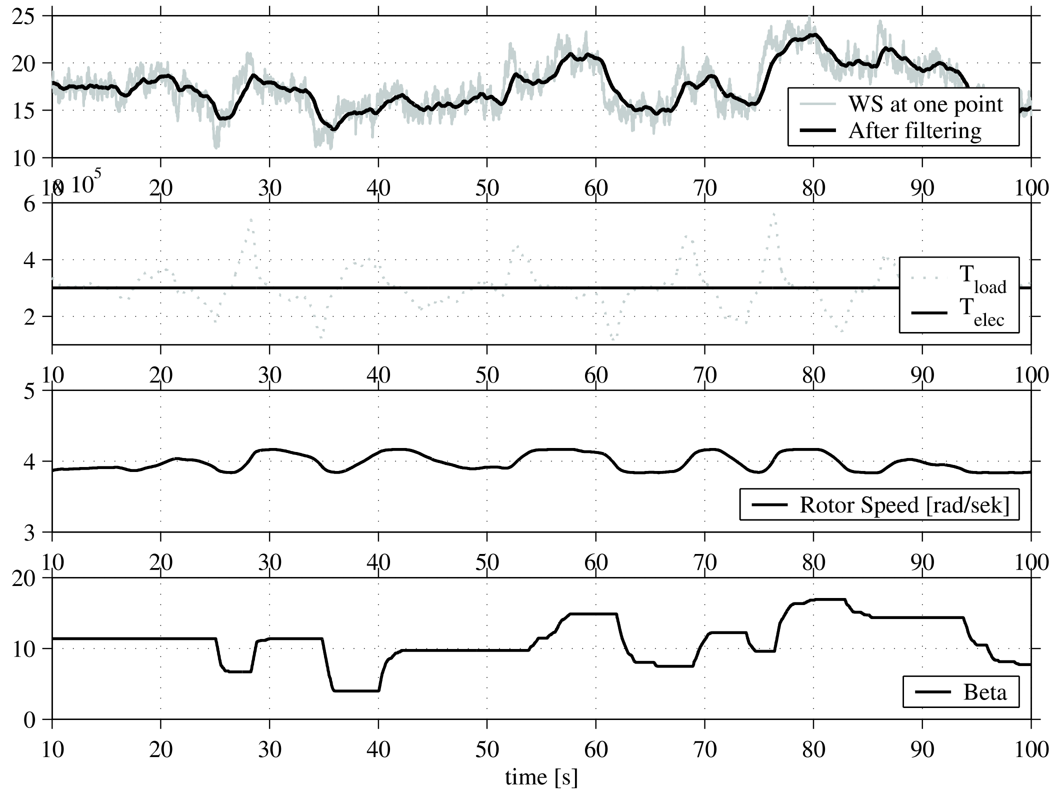

Figure 6.9. High Wind Speed Controller Result

In high wind speed interval in order to limit the input power to the rated one the pitch control is used. In Figure 6.9 and 6.10 pitch actuator activity is shown with used rotational sampling filter and not. We can observe different pitch actuator performance with the same wind condition in both cases. Because the demand of electrical torque is constant the power from wind can be estimated by measure the actual rotor speed. To adjust the pitch angle we compare the rotor speed between actual and nominal and then if the difference is higher than certain margin we activated the pitch mechanism. Due to this certain margin and fluctuating input torque the highest pitch actuator activity can be observed in Figure 6.10.

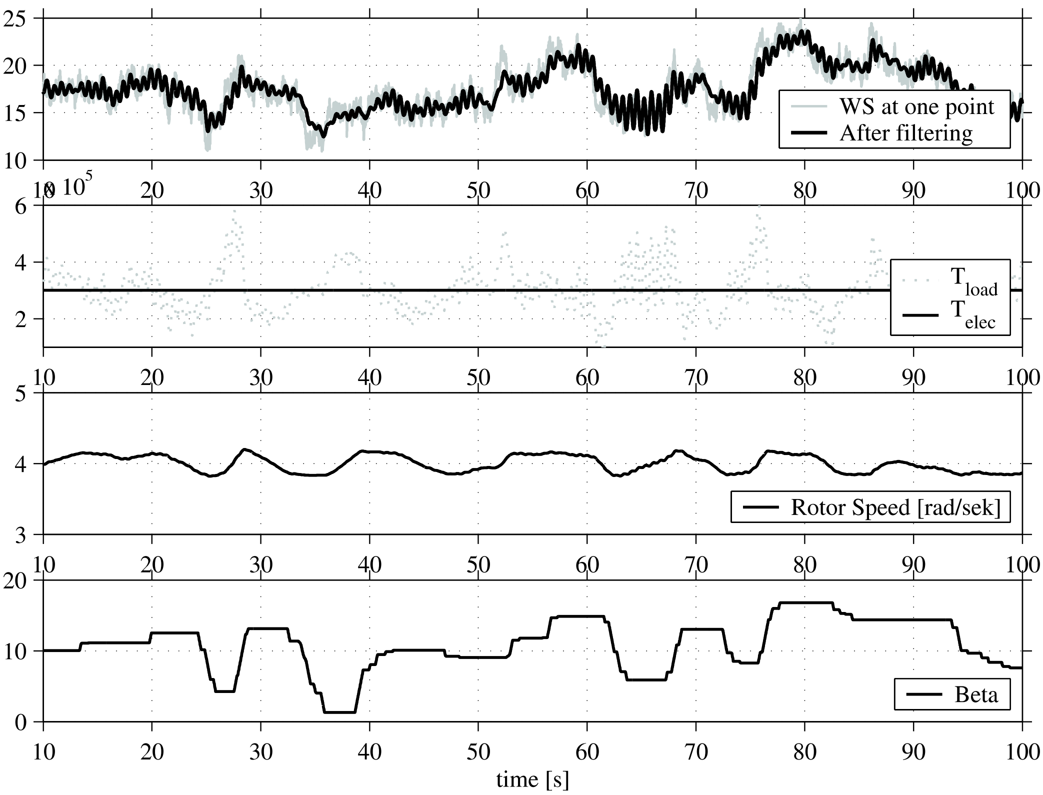

Figure 6.10. High Wind Speed Controller Result with RSF

Chapter 7

Control in The Whole Wind Speed Range

It is not possible to operate in the whole speed area using only one controller and due to this the final controller is a combination of the controllers from the various wind speed intervals. Finally, after modelling and analyzing those three different controllers, the whole control scheme is obtained. First of all, the controllers are combined together using switches, secondly the proper switching criteria have also been developed. There are two criteria which make decision and switch to the proper controller. The control overview scheme is shown in Figure 7.1. As we

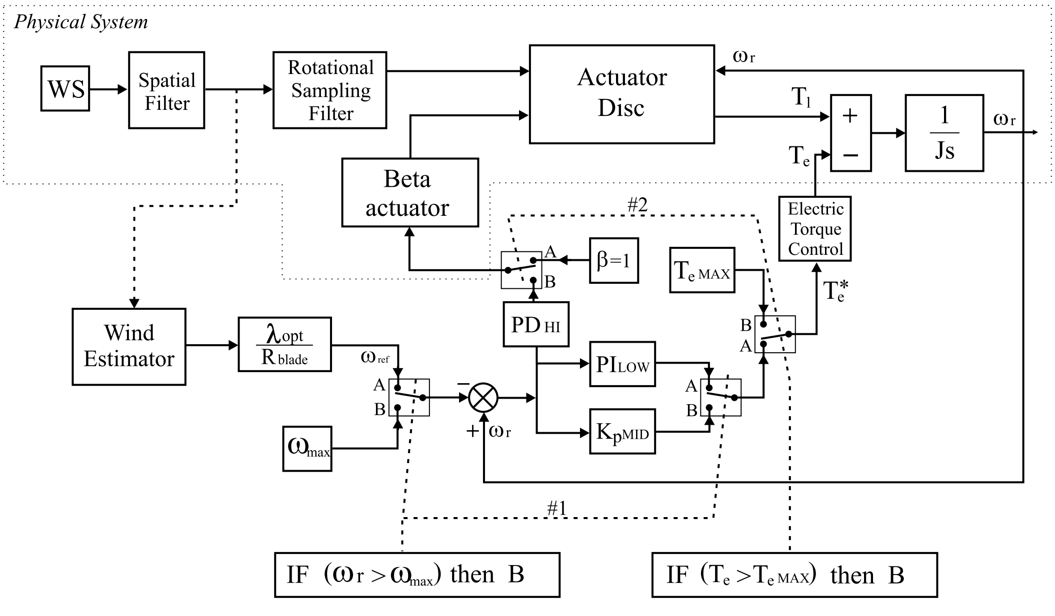

Figure 7.1. Overview of the complete control scheme

can see there are four switches, and two drive signals from the control logic. Each signal switch two switches simultaneously. Using an ordinary switch with "hard" switching in some places is not convenient due to significant signal difference on input connector. In places where during the switching there are no differences in the output, an ordinary switch can be used.

7.1 Switching Approach

To obtain the intended results, three types of switches were implemented. For a smooth torque when switching between region I and II, the switch with proportional characteristic is used. That means, in a certain margin trg the output signal of the switch is the sum of input signals taken with proper proportion. Both input signals are taken with reverse weight, that means if we took 10% of input one, there is accordingly 90% content of input two, and the sum of those signal make up the output value. Switching in that way will cause the output signal to always be continuous, the switching effect will be smooth and the output value will be always between the inputs values. The switching characteristics are shown in Figure 7.2A

In Figure 7.2B is the ordinary switch which is used where during the switching

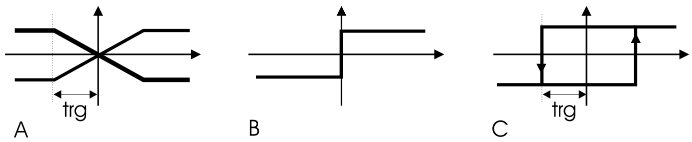

Figure 7.2. Different characteristics of used switches

there are no differences in input. That occur in one of the two switchings which is responsible for the torque demand value between region II and III. In that case even by using an ordinary switch the transient will be smooth due to the criterium. The criterium is set when we reach a certain torque level, and then the switching occur to the value which simultaneous was the criterium level, which didn't cause any discontinuous behavior.

By using the characteristic shown in Figure 7.2C the switch has a hysteresis effect. This switch was used between controller I and II, switching the ω_{ref} value. Using this switch the criterium was much easier to implement, what is seen in Figure 7.4. Using an ordinary switch in this place causing instability and oscillations due to criterium.

The implementation of the switches in Matlab Simulink is shown in Figure 7.3.

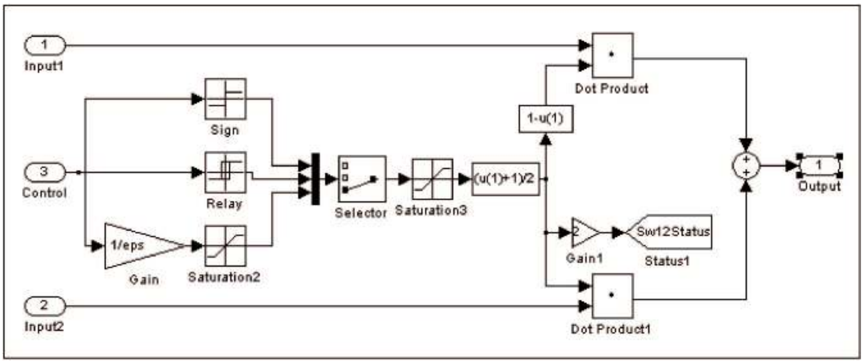

Figure 7.3. Implementation of switches in Simulink

7.2 Establishing the Switching Criterium

There can be several approaches to find a criterium to switch between the operating regions. Each of the regions usually have one fixed parameter and a control variable. In the low wind speed region we have fixed a pitch angle but variable rotor speed and torque demand. If we hit the maximum rotor speed we latch by using a hysteresis switch the ω_{max} value as a reference value (Figure 7.4). In that case the criterium is very simply $\omega_{rotor} > \omega_{max}$ due the switch and the definition of the value when the switch will be back is defined as $\omega_{max} - trg$ where trg is defined inside of switch block.

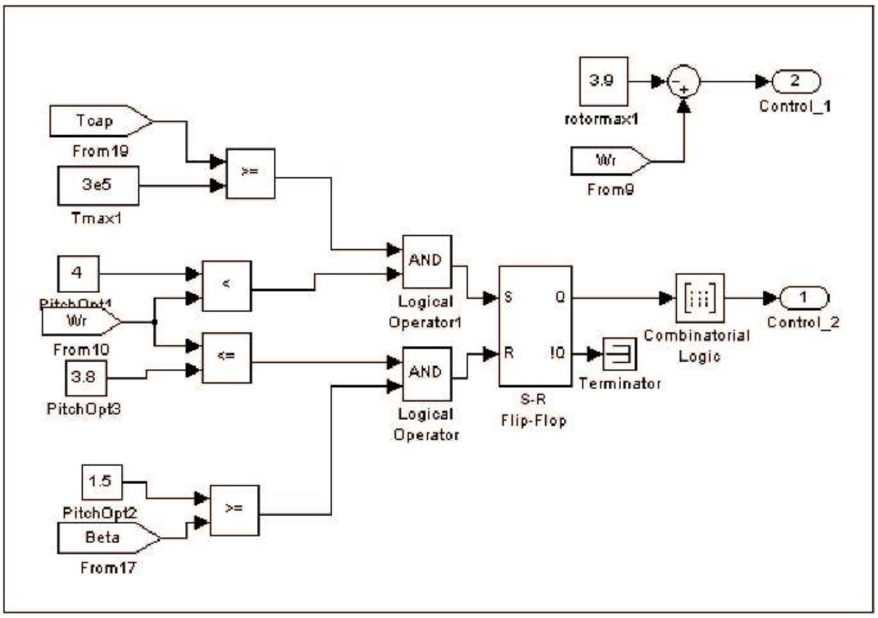

Figure 7.4. Implementation of the switching criteria our wind turbine

The second criterium which switch between the middle and high wind speed interval is more complicated. It uses the R-S flip-flop and two gates. There are different criterium for switching from II to III and different from III to II. When we are in the middle interval, two conditions must be fulfilled in order to pass to switch to region III. First, the rotor speed must be higher than ω_{max} and second, the torque from the wind must be higher than T_{max}. That means that the generated power should be around rated and the pitch control have to be activated. When the wind immediately changed to middle speed, the reset condition on R-S flip flop wait until the pitch angle will be 1 degree and rotor speed, drop to 95% of the ω_{max} value. If that condition is fulfilled the turbine operates in the middle wind speed area which means that, the torque is controlled and the rotor speed is kept at its maximum, and finally the pitch angle is set to the optimum. Instead of a constant output power, like in the high wind speed interval, in this region the power is fluctuating.

7.3 Simulation Result

There are two simulations with different input signals. In Figure 7.5 a linearly increasing wind speed signal from 8 to $16m/s$ is presented in order to to show the result of the switching operations. On the right frame in the top row we see the switch activity and their status. The first higher, continuous line is the switching signal condition between region I and II, the second dotted line is responsible for switching in region II and III.

In the figure showing the torque capture we can observe a small ripple which is caused by the start of the pitching and the finite pitching speed. Also the dead zone on the top of the $C_p(\lambda, \beta)$ table lead to that C_p values on the top are insensitive from pitch angle around $1° - 6°$.

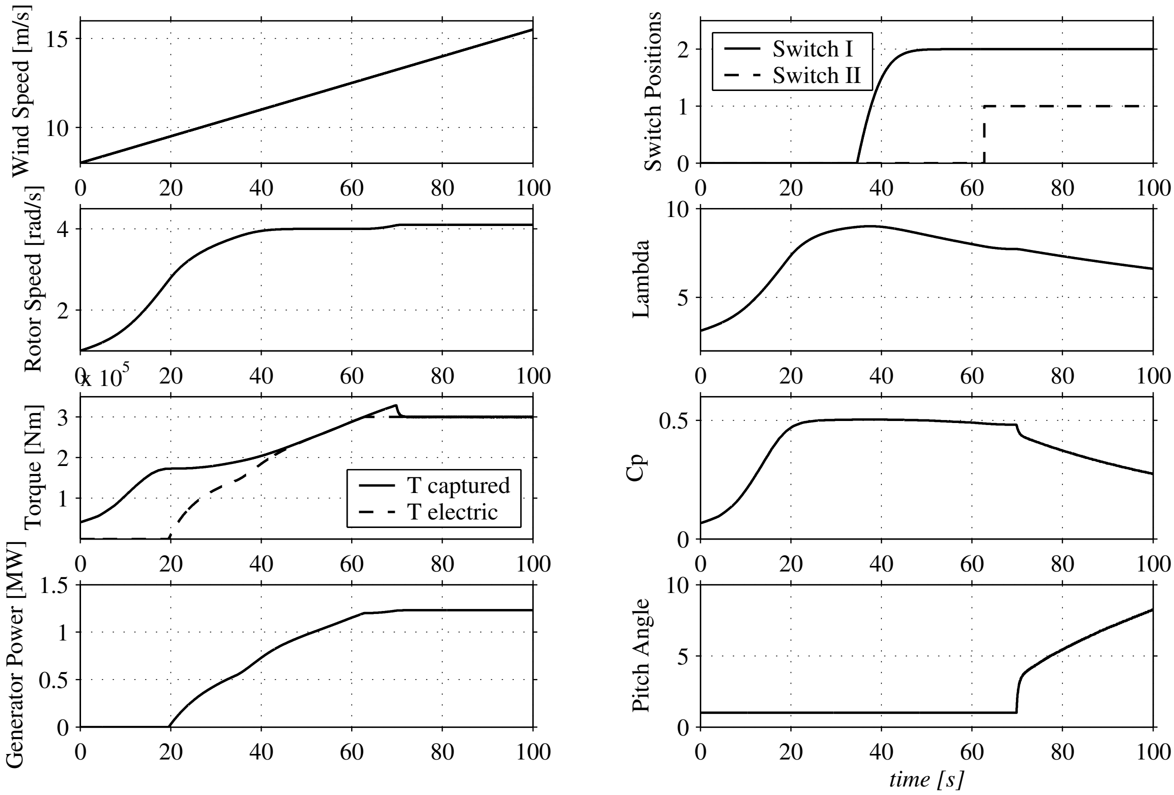

Figure 7.5. Simulation result using as a input linear signal

The second simulation (Figure 7.6) is done using a wide range of wind speeds. On the rotor speed curve we can observe three different behaviors. First when the rotor speed increase exponentially, the turbine is in low wind speed area, then the rotor speed is constant but the power is still below the rated and that means middle wind speed operation. When the rotor speed as well as the torque has reached the maximum, the pitch control is active and we are now operating in the high wind speed area. The pitching speed is set to 8 degree per second as a standard. When the pitching is active we also see that the generated power is around rated, allowing only small variations in the power.

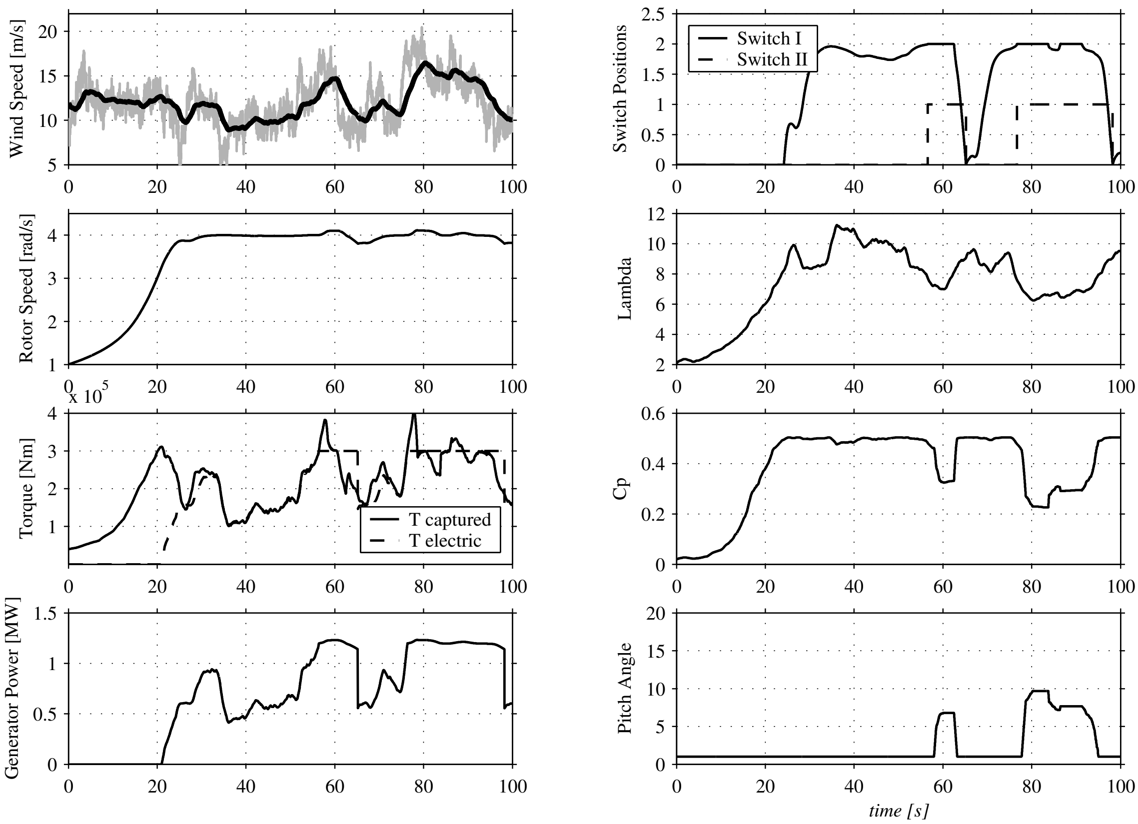

Figure 7.6. Simulation result using syntectic wind speed

7.4 Implementation in Simulink

The whole controller was implemented in Matlab/Simulink (Figure 7.7). The $C_p(\lambda, \beta)$ table was stored in workspace as a matrix. Also several kinds of wind speed series were generated before and stored on disk, which significantly speeded up the simulations.

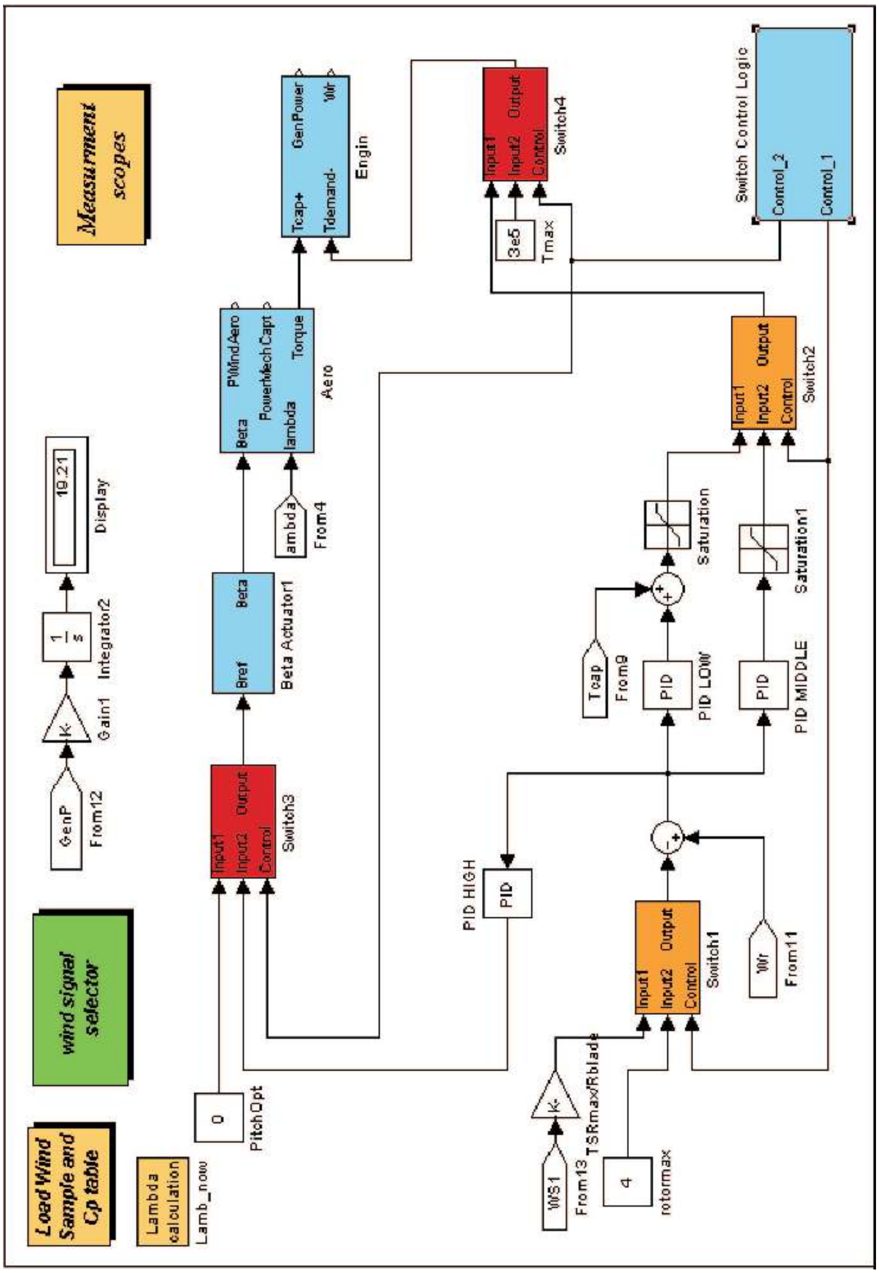

Figure 7.7. Implementation of the whole control structure in the Matlab

Chapter 8

Conclusion

The complexity of the variable speed system leads to increased cost and reduced reliability due to the use of power electronics and a more complicated control. But as a result of using a more advanced control, reduced mechanical stresses on the shaft as well as on the structure of the turbine as well as a better power quality can be achieved. A variable rotor speed turbine allow us to partially store energy from wind gusts in the rotating mass of the turbine rotor instead of transmitting them through the drive train. It is shown that in the low wind speed a controller implementation using a proper tuning a reduction of the mechanical stresses can be achieved without loosing a significant amount of energy (usually by using a slow speed controller).

For the high wind speed interval the crucial part is to have a good pitch actuator, as this is the part responsible for limiting the power in this wind speed region.

For the middle wind speed it also possible to reduce the torque and speed variations by a proper tuning of the PI controller.

It was also observed that, to start pitching the blades in the middle wind speed area can be a good idea as a preparation for high wind speed gusts, otherwise power overshoots may occur.

8.1 Future Work

It would be more correct instead of using a one point wind data series to use a wind field to get more accuracy result. In that case the spatial filter can be avoided. Also estimator for the wind speed and torque is a task for future work.

References

[1] T. Burton, D. Shape, N. Jenkins and E. Bossanyi, Handbook od Wind Energy, John Wiley and Sons LTD, England 2001.

[2] E. Bossanyi, "The Design of Closed Looped Controllers for Wind Turbines", Wind Energy 2000, no. 3. pp 149-163, July, 2001.

[3] T. Thiringer and J. Linders, "Control by Variable Rotor Speed of a Fixed-Pitch Wind Turbine Operating in a Wide Speed Range", IEEE Transaction on Energy Conversion, vol. 8, No. 3, pp 520-526, Sept 1997.

[4] B. Connor and W. E. Leithead, "Performance Assessment of Variable Speed Wind Turbines", Conference on Opportunities nad Advances in International Power Generation, Conf. Public. no. 419, pp 65-71, March, 1996.

[5] H. Vihriala, "Control of Variable Speed Wind Turbine" Ph.D. thesis, Tempare University of Technology, Tempare, Finland, 1998.

[6] T. Thiringer, "Periodic Pulsation from a Three-bladed Wind Turbine", IEEE Transaction on Energy Conversion, vol. 16, no. 2, pp. 128-133, June 2001.

[7] T. Petru, "Modelling of Wind Turbines for Power System", Lic. thesis, Chalmers University of Technology, Goteburg, Sweden, 2001.

[8] S. Heiser, "Wind Energy Conversion Systems", John Wiley and Sons LTD, England, 1998.

[9] E. Persson, "One-dimensional Wind Simulation", Mathematical Statistics, Chalmers University of Technology, Goteborg, 1996.

[10] E. Muljadi and C.P. Butterfiels, "Pitch Controlled Variable Speed Wind Turbine Generation", IEEE Transaction Industry Application, vol. 37, no. 1, pp240-146, Jan. 2001.

[11] K. Pierce and L. J. Fingersh, "Wind Turbine Control System Modelling Capabilities", American Controls Conference, report, June 1998

[12] L. L. Freris, ”Wind Energy Conversion Systems”, Prentice Hall Int., UK, 1990.

[13] T. Thiringer and T. Petru, ”Modelling of Wind Turbines for Power System Studies” IEEE Transaction on Power Systems, vol. 17, no. 4, Nov. 2002.

[14] T. G. Engelen, E. L. Hooft ”Development of wind turbine control algorithms for industrial use” Energy Research Center of the Netherlands, The Netherlands, 2003.

[15] Anca D. Hansen, Florin Iov, Frede Blaabjerg ”Overall control strategy of variable speed double-fed induction generator wind turbine” Nordic Wind Power Conference, 1-2 March, Chalmers University of technology, Goteborg, Sweden 2004.

[16] N. Horiuchi and T. Kwahito, ”Torque and Power Limitations of Variable Speed Wind Turbines Using Pitch Control and Generator Power Control” IEEE Transaction, 2001.

[17] R. Cardenas, G. M. Asher, W. F. Ray, R. Pena, ”Power Limitation in Variable Speed Wind Turbines with fixed pitch angle” Conference on Opportunities and Advances in International Power Generation, Conf. Public. 18-20 March, 1996.

[18] D. Winkelaar, ”Fast three-dimensional wind simulation and the prediction of stochastic blade loads”, Netherlands Energy research Foundation (ECN), Petten, The Netherlands, 1998.

[19] J. F. Manwell, J. G. McGowan and A. L. Rogers, ”Wind Energy Explained”, John Wiley and Sons LTD, Chichester, England, 2002.

[20] D. M. Egglestone and F. S. Stoddard, ”Wind Turbine Engineering Design”, Van Nostrand Reihold Company Inc. New York, USA, 1987.

[21] T. Thringer, ”Measurement and Modelling of Low-Frequency Disturbances in Induction Machines”, Lic. thesis, Chalmers University of Technology, Goteborg, Sweden, 1993.

[22] Mika Rasila, ”Torque and Speed Control of a Pitch Regulated Wind Turbine”, Chalmers University of Technology, Goteborg, Sweden 2003.

[23] E. Muljandi, K. Pierce and P. Migliore, ”Control Strategy for Variable-Speed, Stall-Regulated Wind Turbines”, Proceedings of American Control Conference, vol. 3, pp1710-1715, June 24-26 1998.

Appendix A

Measurement at Jung Turbine

There are three figures showing the power, rotor speed, stator current, stator voltage and pitch angle from Jung turbine in different wind speed intervals. The turbine is Vestas V-52, variable speed, 850kW, placed 100 km far away from the Goteborg, equipped with double-feed induction generator. The measurement presented here(Figure $A.X$) was done in May '04, which was very windy month. The sampling frequency of the stored data was 2048 Hz.

A.1 Measurement at Low Wind Speed (4.5-6 m/s)

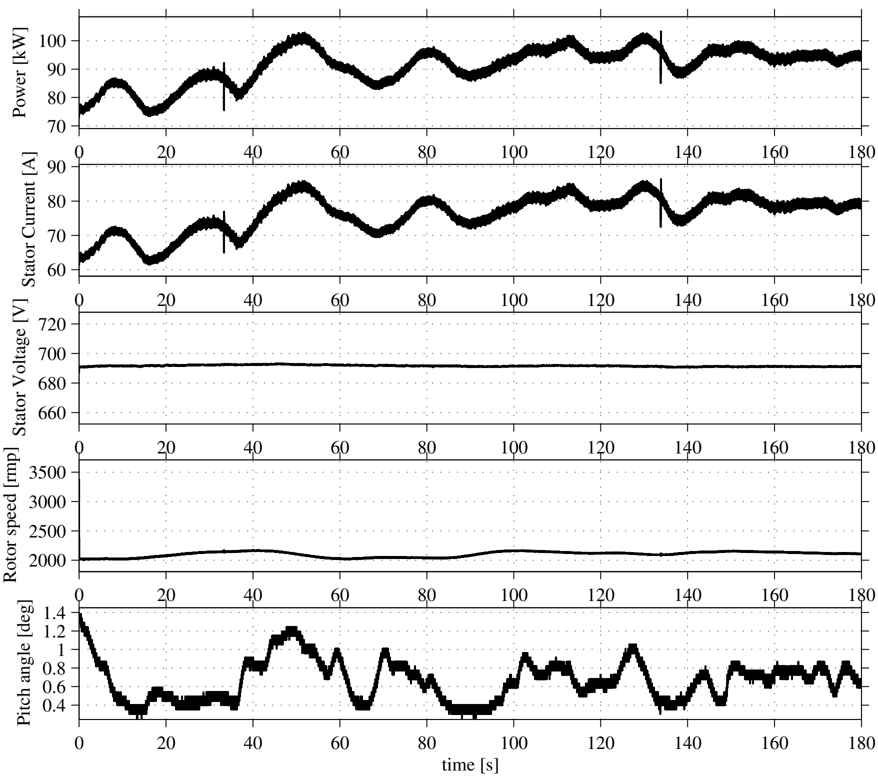

Figure A.1. Measurement at low wind speed in Jung turbine

A.2 Measurement at Middle Wind Speed (8-12m/s)

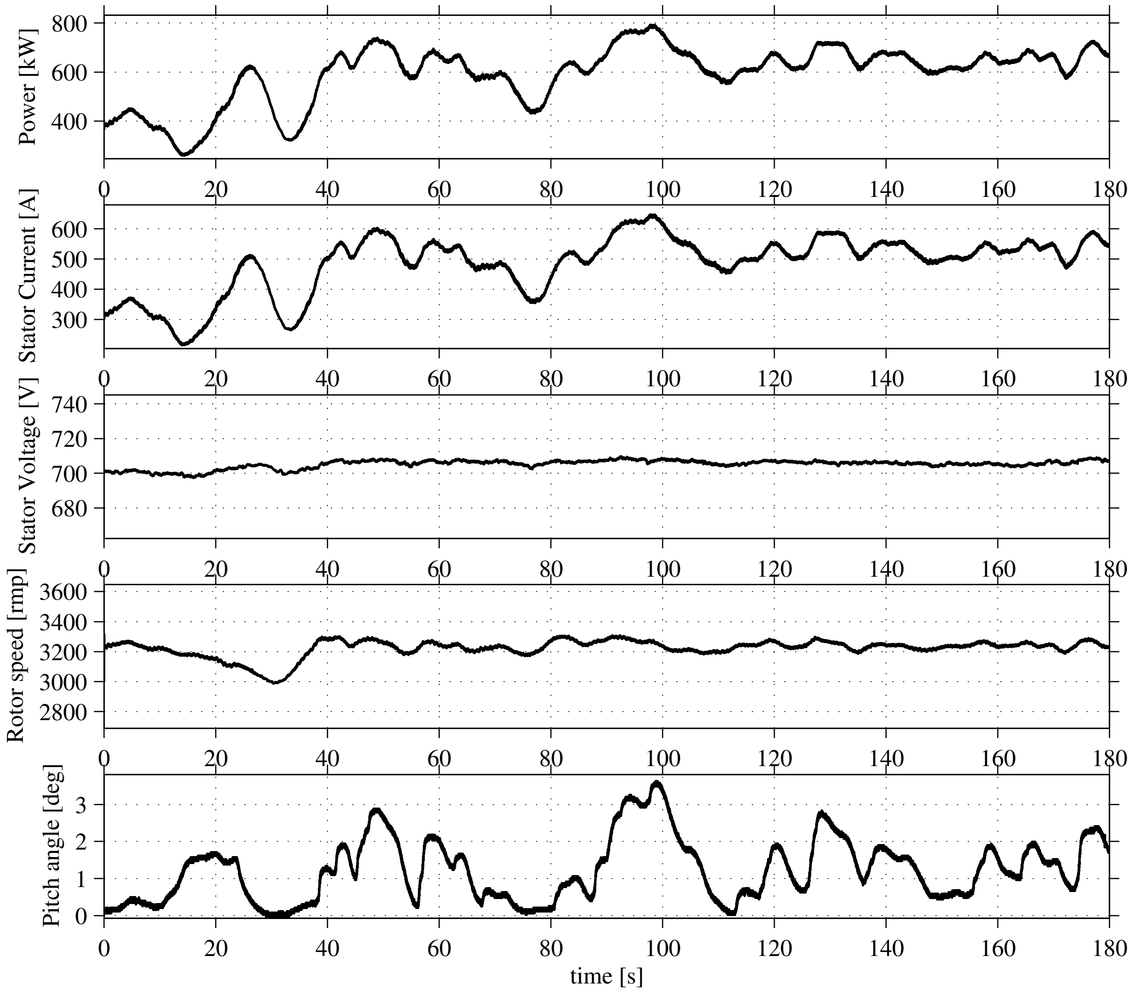

Figure A.2. Measurement at middle wind speed in Jung turbine

A.3 Measurement at High Wind Speed (14 - 23 m/s)

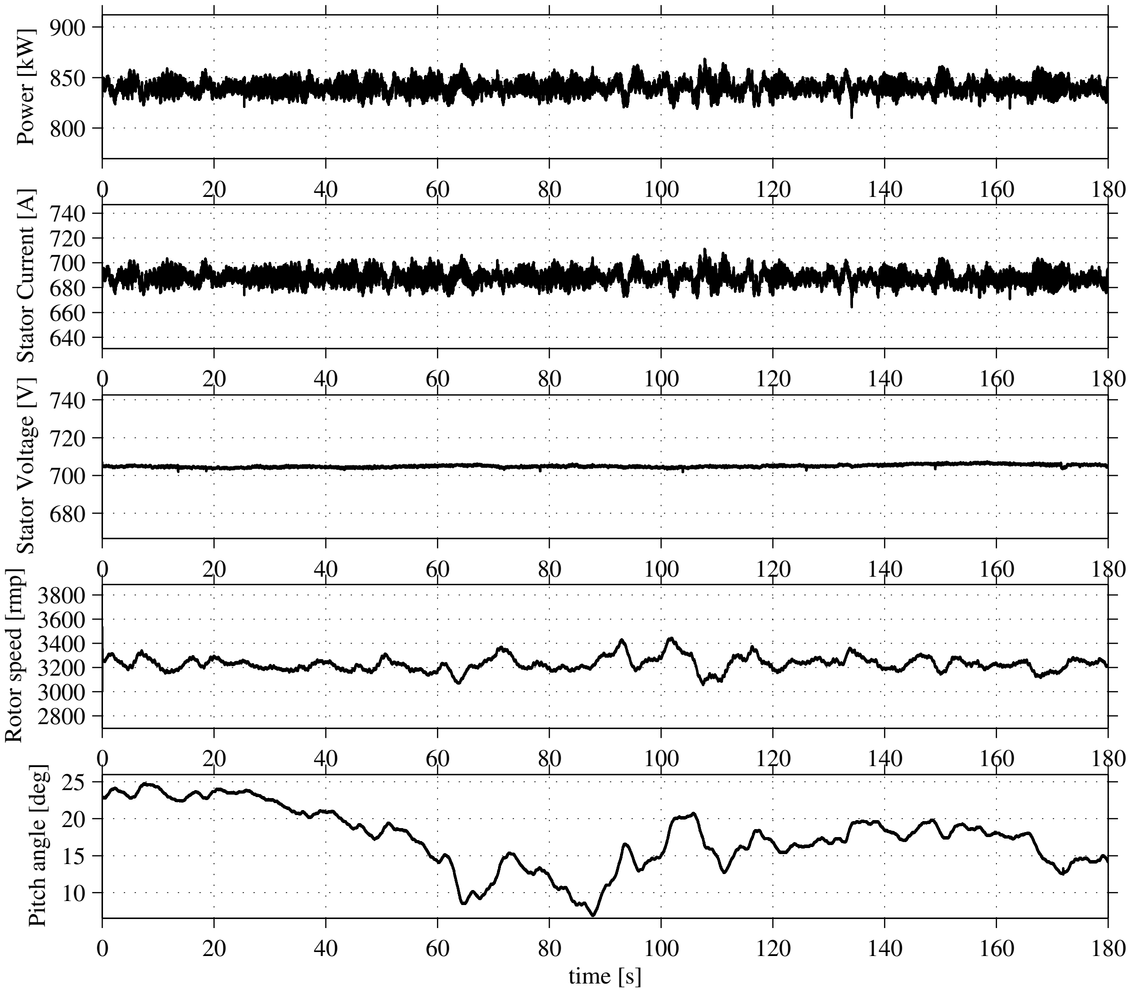

Figure A.3. Measurement at high wind speed in Jung turbine

A.4 Power Spectrum at Different Wind Speed Levels

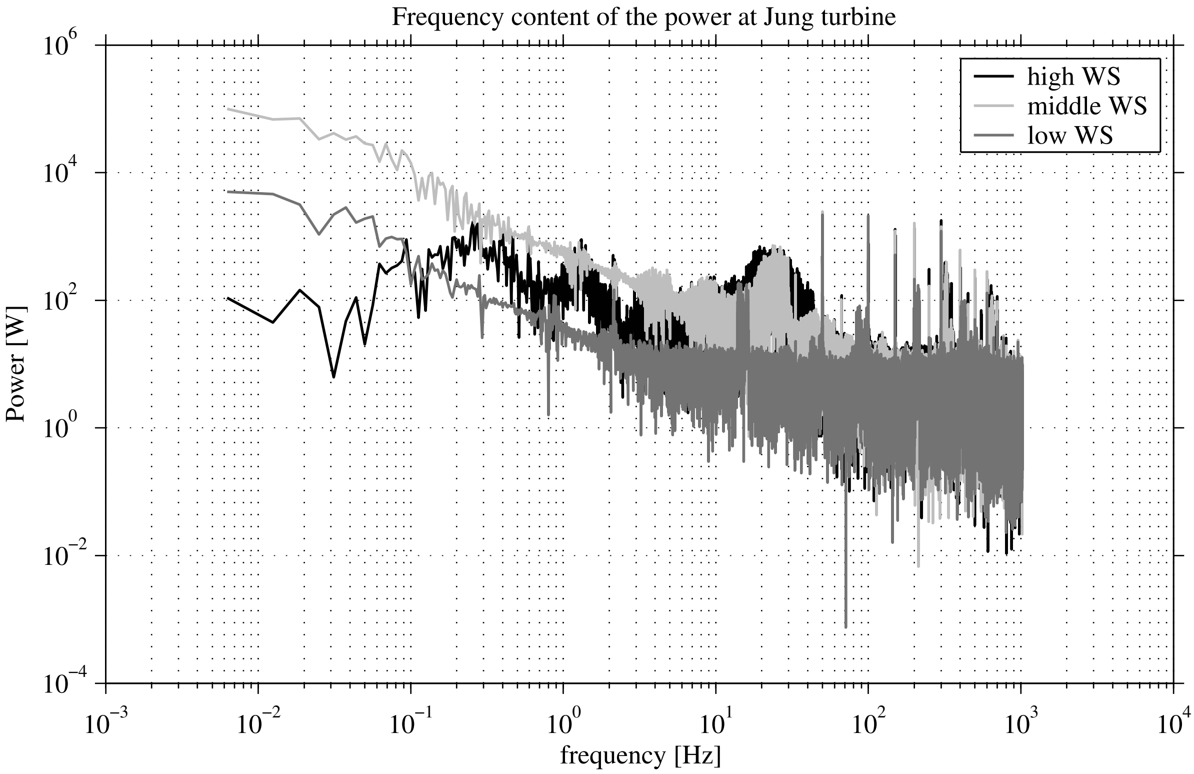

Figure A.4. Spectrum of the power at different wind speed intervals

Appendix B

Measurement at Bast Turbine

The Bast turbine is placed 100 km far away from Göteborg, equipped with gear-less, variable speed, 650kW, permanent magnet generator.

B.1 Measurement at Low Wind Speed

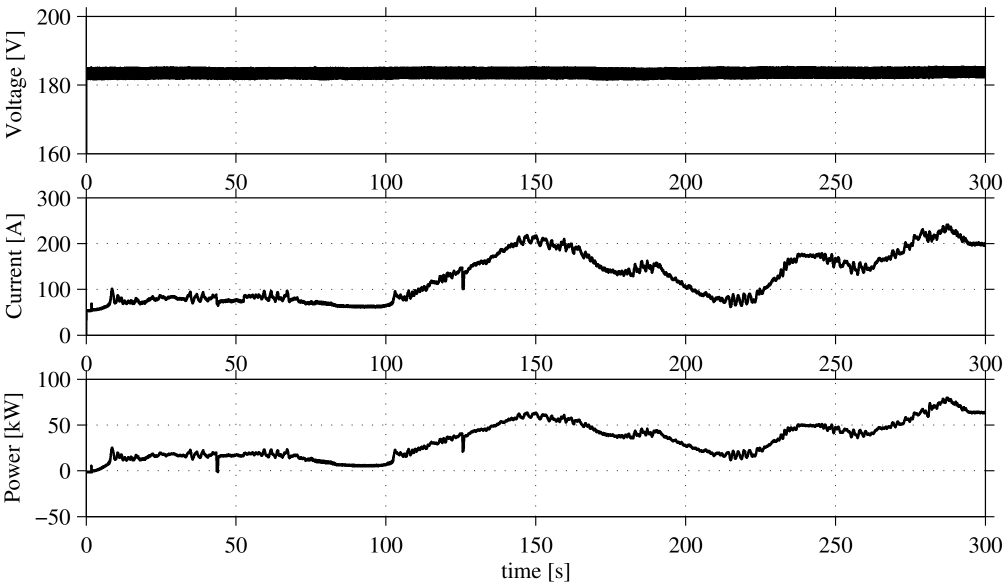

Figure B.1. Measurement at low wind speed in Bast

B.2 Measurement at Middle Wind Speed

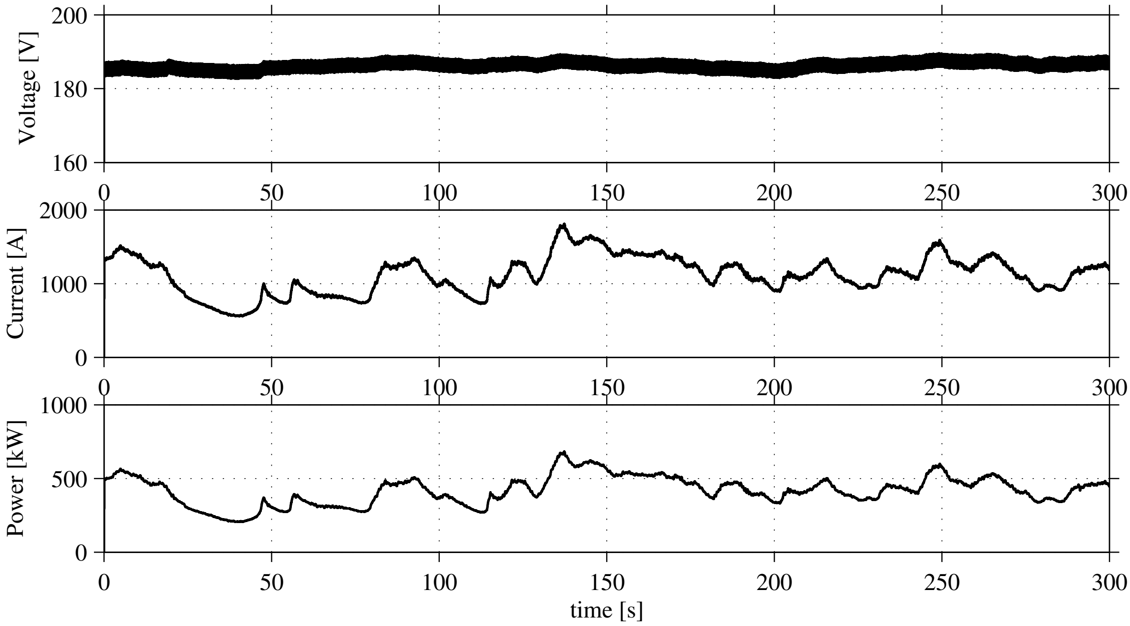

Figure B.2. Measurement at middle wind speed in Bast

B.3 Measurement at Low Wind Speed

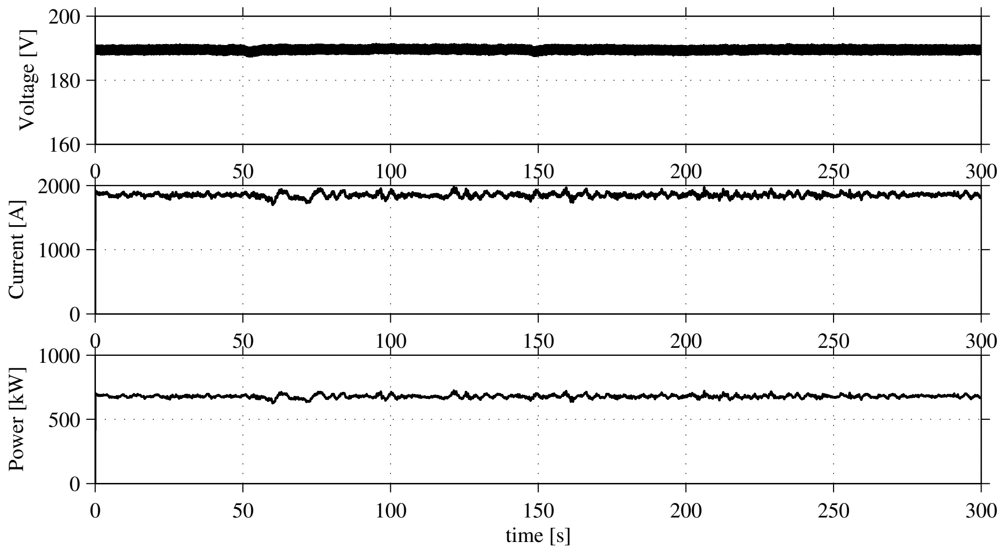

Figure B.3. Measurement at high wind speed in Bast

B.4 Power Spectrum at Different Wind Speed Levels

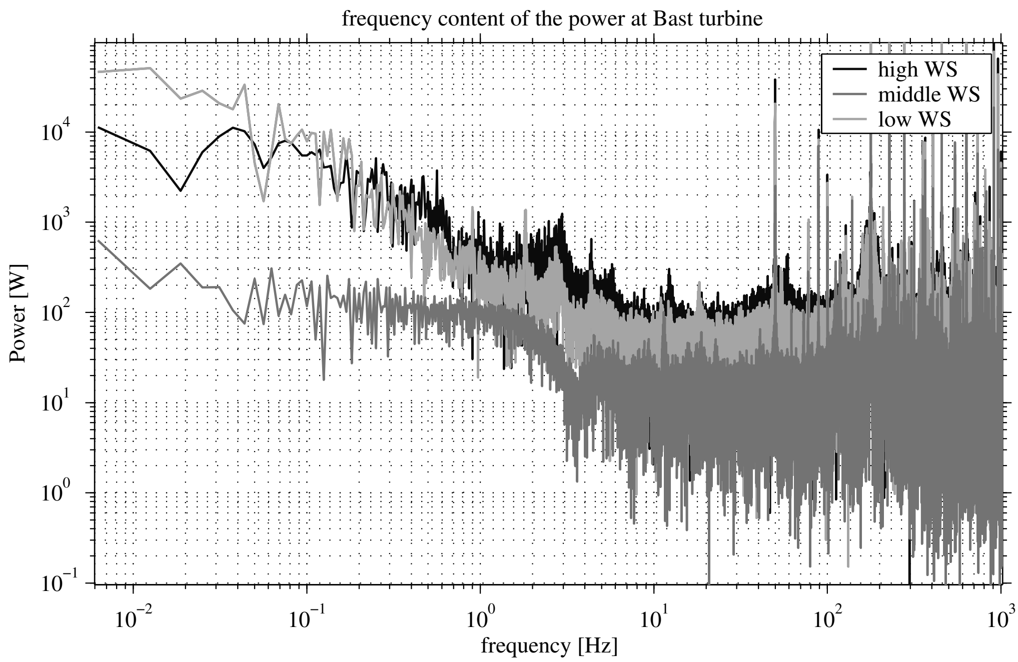

Figure B.4. Spectrum of the power at different wind speed intervals

Appendix C

Simulink implementation

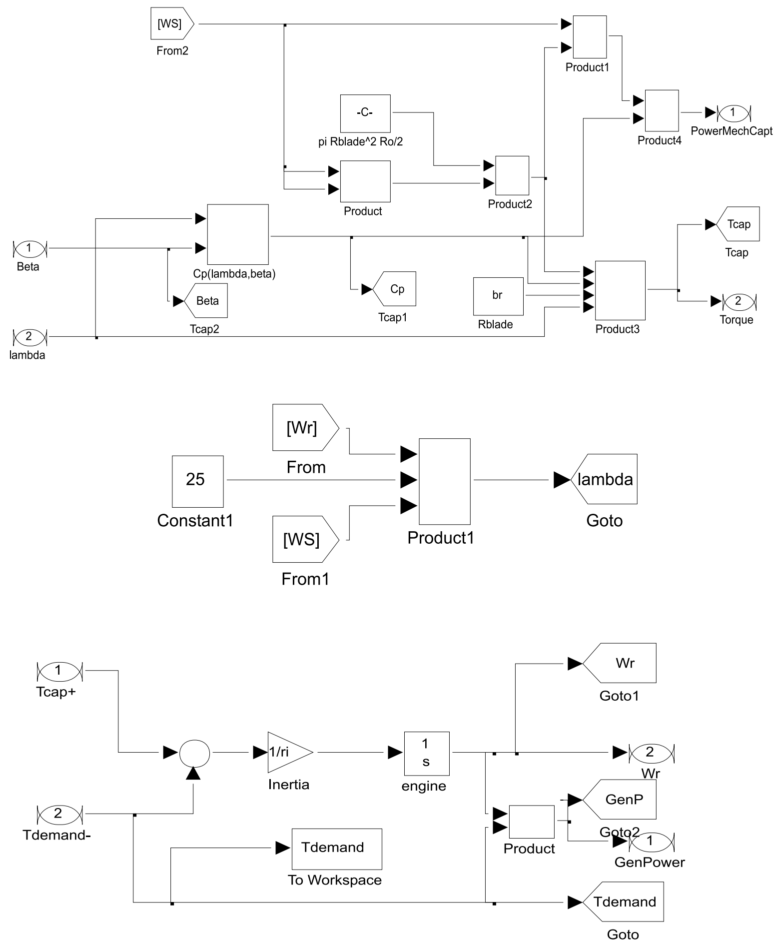

Figure C.1. Physical system - torque from wind calculation and rotor speed with rotor inertia.

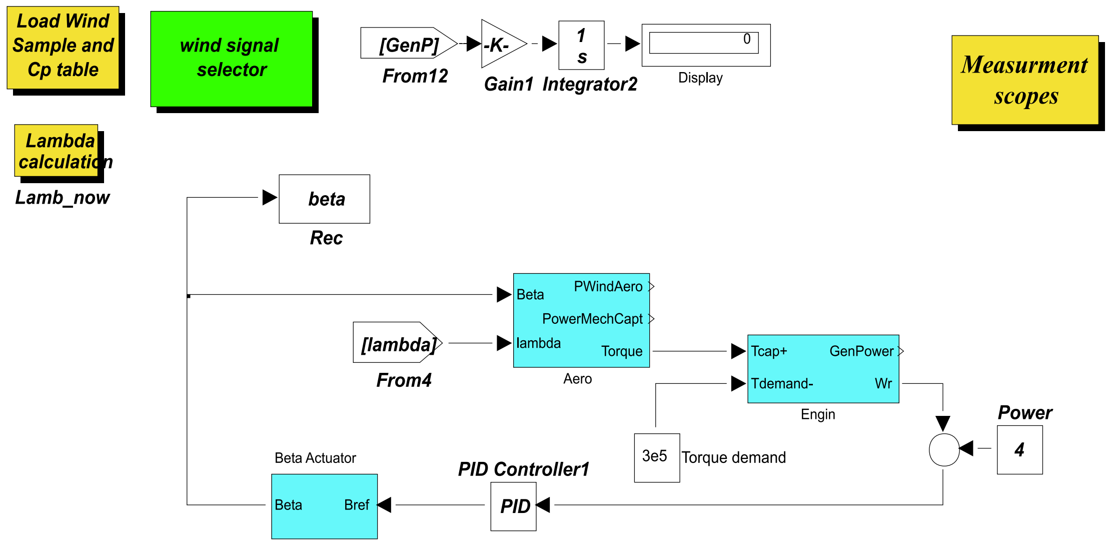

Figure C.2. high wind speed controller

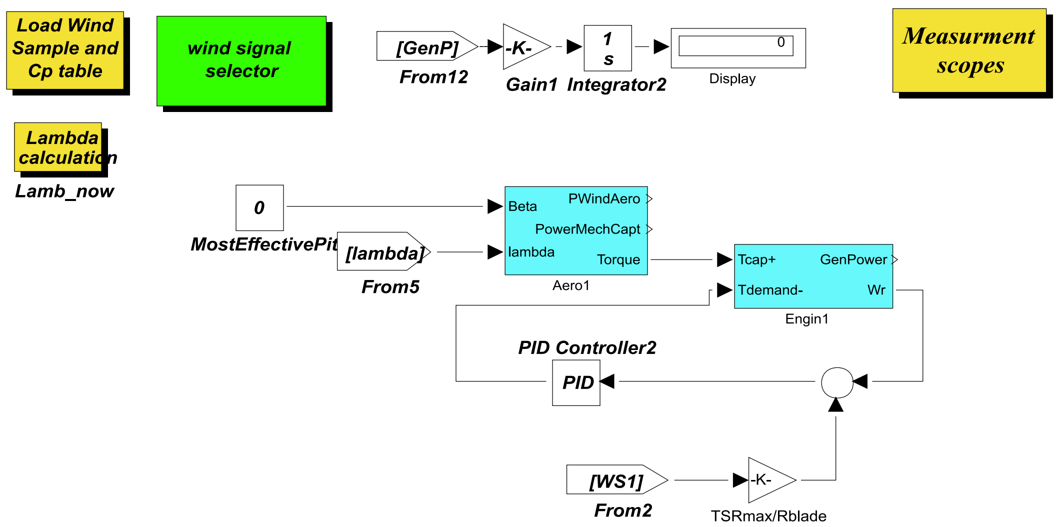

Figure C.3. low wind speed controller

Appendix D

Wind Simulation Program

```
function [ux, uy, tv]=windsim(t,fsamp,fcut,u)

% finish time in seconds
% fsampling sampling speed
% fcut to limit the frequency spectrum somewhere
% u mean wind speed

%  call example
%[ux, uy, tv]=windsim(60,50,15,6.4);

len=round(t*fsamp); lenc=round(t*fcut);

n=rand(1,lenc); m=rand(1,lenc);

ak=sqrt(2*(-log(n))); fik=2*pi*m; kdel=(1:lenc)/t;

z=0.3;
z0=0.5; % forest
%z0=0.00001;    % sea

s=16.8/(log(z/z0)^2)*z*u./((1+33*z/u*kdel).^(5/3)); ex=sqrt(s/t).*ak.*exp(-i*fik);
ey=2*pi*kdel.*sqrt(s/t).*ak.*exp(-i*(fik+2*pi/2));

nn=0:len-1; corr1=exp(-i*2*pi*nn/len); corr2=kdel*t*pi*(1/len-1/(t*fsamp));

ux=u+real(corr1.*(fft(ex,len)+nn.*fft(i*2*corr2.*ex,len)-nn.^2.*fft(2*corr2.^2.*ex,len)));
uy=real(corr1.*(fft(ey,len)+nn.*fft(i*2*corr2.*ey,len)-nn.^2.*fft(2*corr2.^2.*ey,len)));
tv=nn/fsamp;

time=(1:len)*fsamp;
clear uy afft=real(s.*ak.*exp(-i*fik)); bfft=imag(s.*ak.*exp(-i*fik));
var=sqrt(s/t).*ak;

uy(1:length(time))=u; for snurr=1:lenc
%uy=uy+afft(snurr)*cos(2*pi*kdel(snurr)*time)+bfft(snurr)*sin(2*pi*kdel(snurr)*time);
uy=uy+var(snurr)*cos(2*pi*kdel(snurr)*time+fik(snurr)); %%
end plot(tv,ux),grid
```